REVIEW

Check for updates

Chitosan/metal organic frameworks for environmental, energy, and bio-medical applications: a review

Akash Balakrishnan,[a] Meenu Mariam Jacob,[b] Nanditha Dayanandan,[b] Mahendra Chinthala, (iD) *[a] Muthamilselvi Ponnuchamy,[b] Dai-Viet N. Vo,*[c] Sowmya Appunni[d] and Adaikala Selvan Gajendhran[e]

Chitosan/metal–organic frameworks (CS/MOFs) are versatile materials fabricated by conjugating the chitosan (CS) material with metal–organic frameworks (MOFs). The CS/MOFs demonstrated phenomenal features such as higher surface area, porosity, non-toxicity, environmental safety, and ability to form different structures, making them suitable for diverse applications in adsorption, catalysis, membrane separation, supercapacitors, batteries, fuel cells, sensing, food packaging, and biomedical applications, including drug delivery. The different preparation routes for fabricating CS/MOFs are elucidated in detail. The CS/MOFs mostly remove emerging pollutants *via* adsorption and membrane separation. However, CS/MOFs are less explored in supercapacitors, fuel cells, and food packaging. This review highlights the preparation, characteristics, and applications of CS/MOFs for energy, environmental and bio-medical applications. The advantages, disadvantages, and perspectives are also elaborated. The following review is expected to be a useful guide for scientists working on CS/MOFs.

1. Introduction

Metal–organic frameworks (MOFs) are an emerging group of porous materials thoroughly explored in the past few years. MOFs are fabricated *via* effective self-assembly of metal ions with organic ligands *via* strong coordination bonds.[1,2] The major characteristic features of MOFs are their porosity, tailored topologies, lower density, better void volume, and good chemical stability.[3,4] In the MOFs, the well-arranged polycrystalline networks offer reactive sites in the form of metal centers and the ligand's functional group.[5] Potential applications of MOFs include wastewater treatment,[6] adsorption,[7] air pollution treatment,[7] photocatalysis,[8] electrocatalysis,[9] sensors,[10] membranes,[11] fuel cells,[12] supercapacitors,[13] batteries,[14] food packaging,[15] drug delivery,[16] and tissue engineering.[17] MOF-based materials always exhibited greater efficiency with tuneable properties.[18] MOFs are easily processed in various forms like aerogels, hydrogels, thin films, membranes, composites, and fibers.[2,19]

Green or bio-based MOFs are yet another novel porous material. Bio-based MOFs are developed from renewable material sources that are environmentally benign, safe and non-toxic.[20,21] Commonly employed bio-based materials are polysaccharides, amino acids, and peptides.[22] The main advantage of using bio-ligands is the availability of multiple coordination sites and functional groups for binding ions.[23] Other merits include abundance and availability, relatively lower cost, easy preparation routes, surface area, and chirality.[24] In this study, chitosan (CS)/ MOFs are focused on because of their biocompatibility and structural strength. Chitosan (CS) is chosen as a green source due to its availability, unique properties and versatile applications in medicine, energy and the environment.[25–28] Although many research papers have been published on this subject, no comprehensive review paper is available on the preparation, properties and applications of chitosan/MOFs. However, Abdelhamid *et al.* (2022) reviewed preparations and applications of the cellulose based MOFs in the allied areas of environmental remediation, gas purifications, drug delivery and biomedical applications.[2] The potential role of MOFs/cellulose composites in potential wastewater treatment was explored by Bej *et al.* (2023).[29]

[a] *Process Intensification Laboratory, Department of Chemical Engineering, National Institute of Technology, Rourkela, Odisha, 769 008, India. E-mail: chinthalam@nitrkl.ac.in*

[b] *Department of Chemical Engineering, College of Engineering and Technology, SRM Institute of Science and Technology, Kattankulathur, 603 203 Tamil Nadu, India*

[c] *Center of Excellence for Green Energy and Environmental Nanomaterials (CE@GrEEN), Nguyen Tat Thanh University, Ho Chi Minh City, Vietnam. E-mail: vndviet@ntt.edu.vn*

[d] *Department of Chemistry, KPR Institute of Engineering and Technology, Coimbatore, 641 047 Tamil Nadu, India*

[e] *Department of Biotechnology, Vinayaka Mission's Kirupananda Variyar Engineering College, Salem, 636 308 Tamil Nadu, India*

This review paper highlights the significant developments attained by CS/MOFs for medical, environmental and energy applications (Fig. 1). The review briefs the preparation methods and properties of CS/MOFs. The study discusses diverse applications of CS/MOFs, such as the adsorptive removal of dyes, pharmaceuticals, heavy metals, photocatalysis, gas adsorption, membrane separation, supercapacitors, batteries, fuel cells, and packaging. Medical applications like antibacterial properties, drug delivery and tissue engineering are described. Finally, the advantages, disadvantages, and prospects are outlined.

2. Chitosan

Chitosan (CS) is a natural fibrous polymer derivative of chitin N-deacetylation found to be a major constituent of crustaceans such as crabs, prawns, shellfish, shrimps and crawfish

(see Fig. 2a).[30,31] The fabrication of CS from chitin is elucidated in Fig. 2b. CS is an N-acetyl-2-amino-2-deoxy-D-glucopyranose unit possessing β-(1–4) bonds on the linear units.[32] CS has been a wonderful polymer in the last few decades because of its abundance, renewability, biodegradability, biocompatibility, safety, affordability, and mucoadhesion-like properties, as shown in Fig. 2c.[33–36] The chemical and physical characteristics highly depend on the molecular weight, degree of deacetylation, solubility, and degree of crystallinity of CS.[34,35] The degree of deacetylation varies from 70 to 95% and influences the potential applications.[37] The presence of the NH_2 and OH usually determines the functionality of CS.[38] NH_2 can be easily protonated, enhancing the solubility in an acidic solution.[39] Two hydroxyl groups are ascribed to modifying the CS's mechanical properties and solubility.

CS also attracted commercial interest due to its greater nitrogen content than cellulose.[40] The polymeric forms of CS

Akash Balakrishnan

Akash Balakrishnan received his master's degree in Chemical Engineering in 2020 from the SRM Institute of Science and Technology, Chennai, India. Currently, he is pursuing a PhD degree in the Department of Chemical Engineering, National Institute of Technology, Rourkela, India under the supervision of Prof. Mahendra Chinthala. He is working on the development of 3D biopolymer-supported photocatalysts for energy and environmental remediation. His research includes photocatalytic degradation of organic pollutants, production of chemicals, biopolymers and process intensification.

Meenu Mariam Jacob

Meenu Mariam Jacob completed her Master's in Chemical Engineering from SRM Institute of Science and Technology, Chennai, India. She is currently pursuing her PhD in Chemical Engineering under the guidance of Dr P. Muthamilselvi in the Department of Chemical Engineering, SRM Institute of Science and Technology, Chennai, India. She is working on wastewater treatment using adsorption and membrane technologies. Her research interests include wastewater treatment, adsorption, membrane, detection, modelling, and carbon-based materials.

Nanditha Dayanandan

Dr Nanditha Dayanandan received her doctoral degree in Chemical Engineering from SRM Institute of Science and Technology, Chennai, India. Currently, she is working as an Assistant Professor in the same department at the SRM Institute of Science and Technology, Chennai, India. Her research interests include membrane technology, membrane distillation, polymeric nanocomposites and wastewater remediation.

Mahendra Chinthala

Dr Mahendra Chinthala obtained his doctoral degree in Engineering Sciences from Homi Bhabha National Institute (Indira Gandhi Centre for Atomic Research), Kalpakkam, India in 2016. He is currently working as an Assistant Professor and leading the Process Intensification laboratory at the Department of Chemical Engineering, National Institute of Technology, Rourkela, India. His research interest includes electrodialysis, electrochemical separations, ion exchange, adsorption; advanced oxidation processes, gasification of biomass, and chemical process simulation using ASPEN PLUS.

are derived semi-synthetically from amino polysaccharides that possess unique properties, functionality and specific applications in the biomedical field.[41] The flexibility offered by this bio-inspired material in creating bonds with the organic and inorganic compounds is because of its functional groups.[42] Studies also claimed that CS and its derivatives display better applications because of their good solubility (water and other solvents). Conversely, chemically treated CS offers higher solubility in commonly used solvents. Furthermore, CS can be formulated into any desired shape or structure, such as powder, bead, membrane and scaffolds (see Fig. 3a). The important applications of CS (see Fig. 3b) include water remediation,[43] catalysis,[44] medicine,[45] agriculture,[46] textile,[47] cosmetics,[48] paper industry,[47] food industry,[28] drug delivery,[33] and nanotechnology.[49]

3. Metal–organic frameworks

Metal–organic frameworks (MOFs) or porous coordination polymers are a prominent group of highly crystalline microporous materials developed based on principles of coordination chemistry.[1] MOFs are formulated based on the self-assembly of organic linkers and coordination nodes of the metal ions or the cluster of metal ions.[50] Metal ions such as aluminium, copper, zinc, titanium, magnesium and zirconium are used to fabricate MOFs.[51] The MOFs can be developed into morphologies like 1, 2 and 3 dimensional structures.[52] The main structural characteristics of MOFs are their phenomenal porosity of 90% for their free volume and greater internal surface area ($>10\,000$ m^2 g^{-1}).[1,53] These properties make MOFs perfect

Dr Muthamilselvi Ponnuchamy completed her PhD from SRM Institute of Science and Technology, Chennai, India in 2016. Currently, she is working as an Assistant Professor in the Department of Chemical Engineering, SRM Institute of Science and Technology, Chennai, India. Her research interests include wastewater treatment, membrane technology, and utilization of waste to wealth and process control.

Muthamilselvi Ponnuchamy

Dr Dai-Viet N. Vo received his PhD degree in Chemical Engineering from The University of New South Wales (UNSW), Sydney, Australia in 2011. He was a postdoctoral fellow at UNSW and Texas A&M University, Doha, Qatar. He was a Senior Lecturer at University Malaysia Pahang, Malaysia from 2013-2019. Dr Vo is currently the Deputy Director of Institute of Applied Technology and Sustainable Development, Nguyen Tat Thanh University, Ho Chi Minh City, Vietnam. His research area is the production of green synthetic fuels via Fischer–Tropsch synthesis using biomass-derived syngas from reforming processes. Dr Vo is the Assistant Subject Editor for the International

Dai-Viet N. Vo

Dr Sowmya Appunni received her PhD degree in Chemistry from the Gandhigram Rural Institute – Deemed University, India. She worked as a postdoctoral fellow and research associate at the SRM Institute of Science and Technology, Chennai, Tamil Nadu, India. Dr Sowmya is currently the Assistant Professor at the Chemical Engineering Department, KPR Institute of Engineering and Technology, Tamil Nadu, India. She is a dedicated researcher with teaching experience in chemistry and research expertise in various water treatment technologies, material chemistry especially polymers and composites; nanoparticles, photocatalysts, and sensors.

Sowmya Appunni

Adaikala Selvan Gajendhran completed his master's degree in biotechnology from Bharathidasan Institute of Technology Campus, Anna University, Tiruchirappalli, Tamil Nadu. Now, he is working as an Assistant Professor in the Department of Biotechnology, Vinayaka Mission's Kirupananda Variyar Engineering College, Salem, Tamil Nadu, India. His research interests include applied microbiology, drug delivery and biofuels.
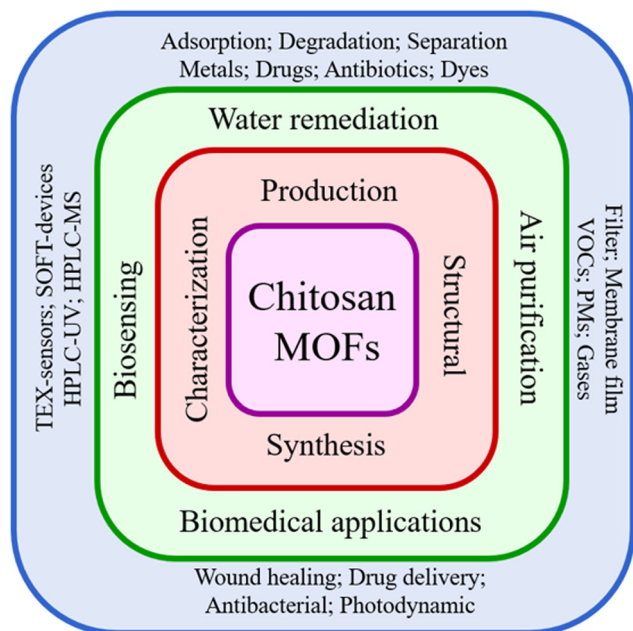
Adaikala Selvan Gajendhran

Fig. 1 An overall summary of the topics reviewed in this study. The important applications include wastewater treatment, air purification, sensing, food packaging, biotechnology and biomedical applications.

materials for adsorption,[54] photocatalysis,[55] supercapacitors,[56] batteries,[57] sensors,[52] and biomedical applications.[58] As per the Cambridge structure database, about 70 000 structures of MOFs are available. Commonly reported MOFs (see Fig. 4) are zeolitic imidazolate frameworks (ZIF),[59] Universiteteti Oslo (UiO-66),[60] Hong Kong University of Science and Technology (HKUST-1),[61] and Materials for Institute Lavoisier (MIL-53).[62] The advantages of MOFs are their phenomenal surface area and porosity, size selectivity, good optical properties, mechanical and thermal stability, higher density of transition metals, and capability to control the compositions and structure of MOFs.

The disadvantages include (i) their lower electrical conductivity, (ii) the poor recovery and reusability of the powdered MOFs are undesirable for several applications including water remediation, and (iii) their higher fabrication costs and lower stability always hinder the utilization in large-scale operations.

4. Chitosan/MOFs

The formation of biopolymer/MOFs is a promising solution to surmount the hereditary restraints related to the stability and recyclability of the MOFs.[23] Several researchers stressed the conjugation of different biopolymers like CS, cellulose, and cyclodextrin onto the MOFs. The hybrid materials prepared using CS and MOFs displayed the characteristics of both CS and MOF, along with the new properties formed via strong interaction between MOFs and CS as indicated in Fig. 5.[25] In most cases, hybrid materials are stabilized by appropriate complexation between the MOF's metal center and CS's functionality. The diagrammatic representation of CS/MOF is shown in Fig. 5. The inclusion of CS with MOFs resulted in exceptional stability, better optical properties, conductivity, adsorption capacity, flexibility and mechanical properties. The important advantages of CS/MOFs are depicted in Fig. 5.

4.1 Design criteria for CS bio-polymeric ligand in MOFs

The preparation of MOFs involves metal ions and an organic ligand responsible for forming coordination bonds, yielding a crystalline structure with greater surface area and better efficiency.[64] Several MOF types are reported for diverse sector applications.[65] Recently, CS-based MOFs have emerged from combining MOF-based chemistry and science.[66] Even though exact definitions for bio-MOF or CS/MOFs do not exist, two different aspects are highlighted in the literature: (a) inclusion of a biomolecule as a ligand in the development of MOFs, and
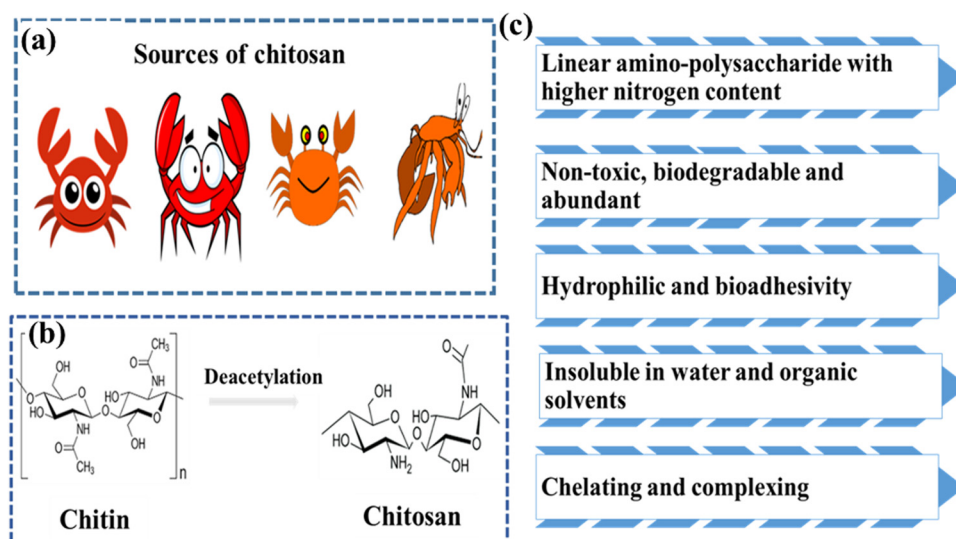

Fig. 2 (a) Natural sources of CS such as crab shells, shellfish and prawns, (b) deacetylation of chitin into CS, and (c) important properties of CS such as environmental suitability, biodegradability, and hydrophilic nature etc.
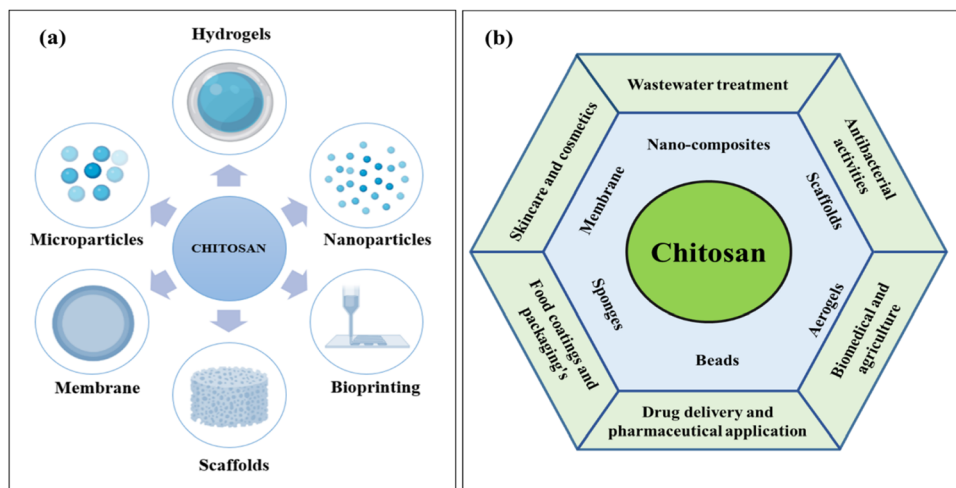
Fig. 3 (a) Different formulations of CS into hydrogels, nano–particles, membranes, scaffolds, and bio–printing, and (b) applications of CS–based materials in the field of environment, medicals and food packaging.

(b) greater porosity after incorporating a natural material.[23] Including bio-inspired materials may attribute new features and extend their applications to other fields. As a result, some strategies are proposed to yield highly efficient CS/MOFs.[67]

• Utilization of CS as one of the organic ligands during the preparation of MOFs.

• The formation of composites *via* covalent coupling with the MOF linkers through post-preparation strategies.

• CS is also used as a bio-ligand, and it may ensure the biocompatibility, crystallinity, and functionality of the prepared CS/MOFs.

4.2 Synthesis of CS/MOFs

The CS/MOFs can be developed through *in situ* and *ex situ* strategies (Fig. 6). The *ex situ* method involves the inclusion of prepared MOFs into the respective form of CS. The *ex situ* approaches include direct mixing, and immersion coating. In direct mixing, MOFs are directly mixed with a CS solution (Fig. 7a). In the immersion coating, the CS-based template or scaffolds is immersed into the solution containing MOF particles. The main advantages are the ability to control MOFs loading with CS, better surface area and greater adsorption capacity. Still, this method is highly time-consuming and requires several chemicals.[2]

In the *in situ* approach, MOF precursors are directly added to the CS-based materials.[2] The respective precursors are usually added to the unprocessed CS materials. Furthermore, the processed CS matrix undergoes freeze–drying to develop CS/MOF aerogels. Freeze drying is the simplest approach to yield porous composites. The yielded CS/MOF aerogel is a three-dimensional porous network cross-linked *via* van der Waals forces and hydrogen bonds.[68] Different parameters like the CS to MOF ratio, concentration, and freezing rate define the stability and porous structure of aerogels. The crystallinity, porosity, and suitability of the CS/MOF aerogel make it suitable for diverse applications in water treatment.

The step *in situ* growth is the step-wise exposure of the MOF precursor with the CS solution (Fig. 7b). The addition of MOF

precursors forms the effective coordination bond between the CS. Later, the inclusion of organic linkers initiates nucleation and growth.[69] The layer-by-layer method is the *in situ* route in which the CS substrate is appropriately submerged in the metal-ion solution (Fig. 7c). It is subsequently submerged in the organic ligand solution and *vice versa*.[70] Homogeneous morphology and controlled thickness are offered by this method. The *in situ* growth is related to the step-wise exposure of the CS substrate to the respective MOF precursor. Initially, inclusion of the metal precursor forms an initial coordination between the metal ions and the functional groups of the CS. Finally, the organic linkers are added for nucleation and growth. Advantages of *in situ* methods include (i) a simple preparation route, (ii) better mechanical properties, (iii) better interaction between polymer and MOFs, and (iv) the ability to control the morphology and homogeneous distribution of MOFs.[71] However, the precise control of the MOF loading on the CS is relatively complicated in the *in situ* strategy.

4.3 Processing of CS/MOFs

The CS/MOFs are easily formulated into different forms like aerogels, foams, hydrogels, thin films, and membranes. Methods like casting, dip-coating, electrospinning, filtration, and 3D printing can be adopted for the same, as illustrated in Fig. 8. Some of the methods are explained below:

(a) Filtration is one of the most-simple fabrication routes that have attained phenomenal research interests in the last decade. The CS/MOFs suspension's solvent permeates through the membrane filter with the help of a vacuum. Finally, the CS/MOFs symmetrical structure is attained after drying. The merits of this method include high flexibility, permeability and porosity.

(b) Casting is a widely used method to build up Bio-MOFs mixed membranes. The matrix solution (preferably CS/MOFs solution) is poured slowly into a glass plate, followed by degassing, solvent extraction and drying. The formed membrane can be peeled off from the glass plate. Generally,
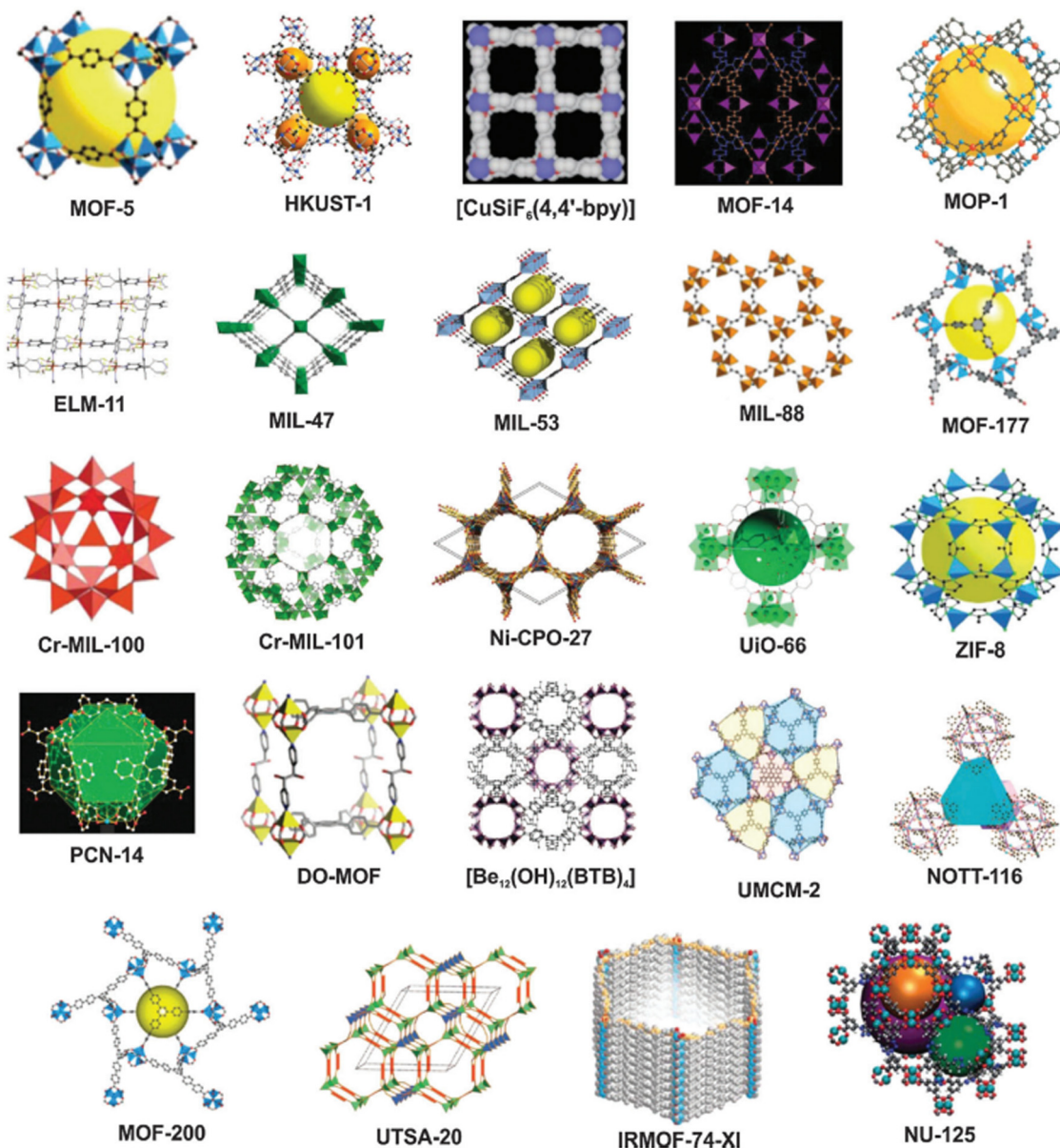
Fig. 4 Structures of different MOFs. The Commonly employed MOFs are ZIF-8, MIL-53, HKUST-1 and MIL-53. Reproduced with permission.[63] Copyright 2015, Royal Society of Chemistry.

the prepared membranes show greater permeability which is useful in water remediation and separation of gases.[69]

(c) Immobilization: the MOFs nanoparticles are immobilized on the surface of CS networks *via* crosslinking, encapsulation, *etc.*[72] This method is highly useful for preparing CS/MOFs beads. It is also beneficial to avoid the loss of nanoparticles and improve reusability.[73]

(d) 3D printing: 3D printing is a trending strategy for preparing CS/MOFs. Major steps include CS/MOFs ink preparation, object structure design, and development upon computer-driven digital controller *via* a layer-by-layer strategy.[74] 3D printing offers greater reproducibility, low cost, easy scale-up, and porous structures.[75,76]

(e) Electrospinning: one-dimensional materials like fibers using polymers and MOFs precursors can be prepared using electrospinning.[77] This route includes the preparation of nanofibers.[78] The voltage is applied to the liquid stream and collector, allowing movement *via* a nozzle. Lastly, fibers are deposited at the collector after drying.[31,73]

(f) Freeze–drying is used to yield a highly porous CS/MOF composite. The freezing of the CS/MOFs is conducted at a lower temperature than the freezing point of a liquid. The aerogel is yielded from the sublimation of frozen small molecular solvents by means of liquid nitrogen freeze–drying methods.[79] Freeze drying yields a three-dimensional porous network structure cross-linked *via* physical interactions like hydrogen bonds, chain entanglements, and electronic associations. The yielded aerogel exhibits high crystallinity and porosity and makes it suitable for diverse applications.[69]
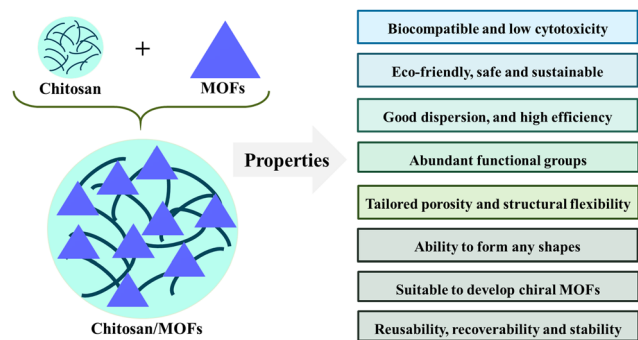
Fig. 5 Diagrammatic representation of CS–MOFs and their important advantages make them suitable for diverse applications.

5. Applications of CS MOFs

In the upcoming topics, we thoroughly explore the diverse uses of CS/MOFs. The broad applications of CS/MOFs include adsorption, catalysis, sensors, and membranes. The biomedical applications are explained with respect to wound healing, antibacterial, tissue engineering and drug delivery.

5.1 Adsorptive removal of pollutants

Adsorption is the most used wastewater remediation tool for treating the effluents seen in wastewater.[80–82] The adsorption is highly preferred due to its easiness in operation, selectivity, cost-efficiency, and flexibility.[83] However, adsorption poses several problems connected to the appropriate disposal and regeneration of CS/MOFs.[84] Several researchers reported eliminating dyes, heavy metals, pesticides, phenols, and pharmaceuticals using CS/MOFs.
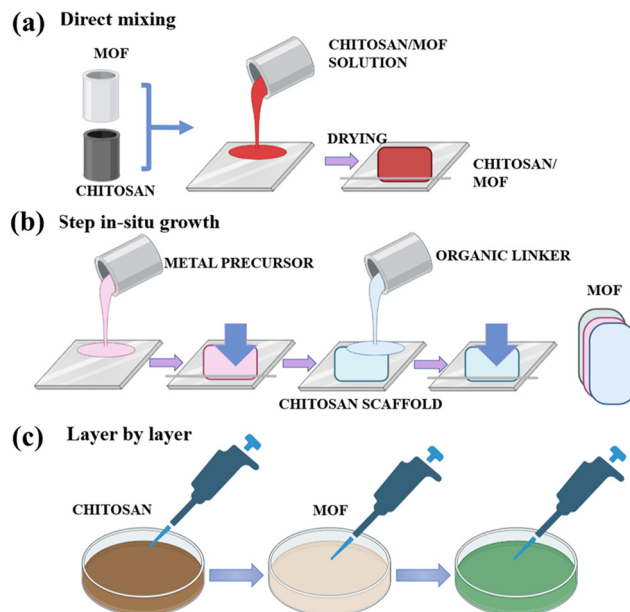
Fig. 7 Schematic representation of different preparation strategies like (a) direct mixing, (b) step-wise *in situ* growth and (c) a layer-by-layer strategy for the preparation of CS/MOFs.

5.1.1 Dyes. Dyes are well-known coloured complex structures that exhibit affinity towards the substrates they applied.[85,86] Almost forty thousand different dyes are available worldwide with an annual production of 45 000 tons. Nearly 15% of these various dyes are directly discharged into the water through synthesis and application.[31] Dyes are commonly employed in industrial sectors like textiles.[87] Additionally, these dyes cause adverse health effects such as breathing problems,

Fig. 6 Fabrication of CS/MOFs using different methods.

allergies, eye and skin disorders, and tissue necrosis.[31,88] The growth of aquatic organisms is also hindered due to dyes and residues such as amines and imines in the marine environment.[31,89]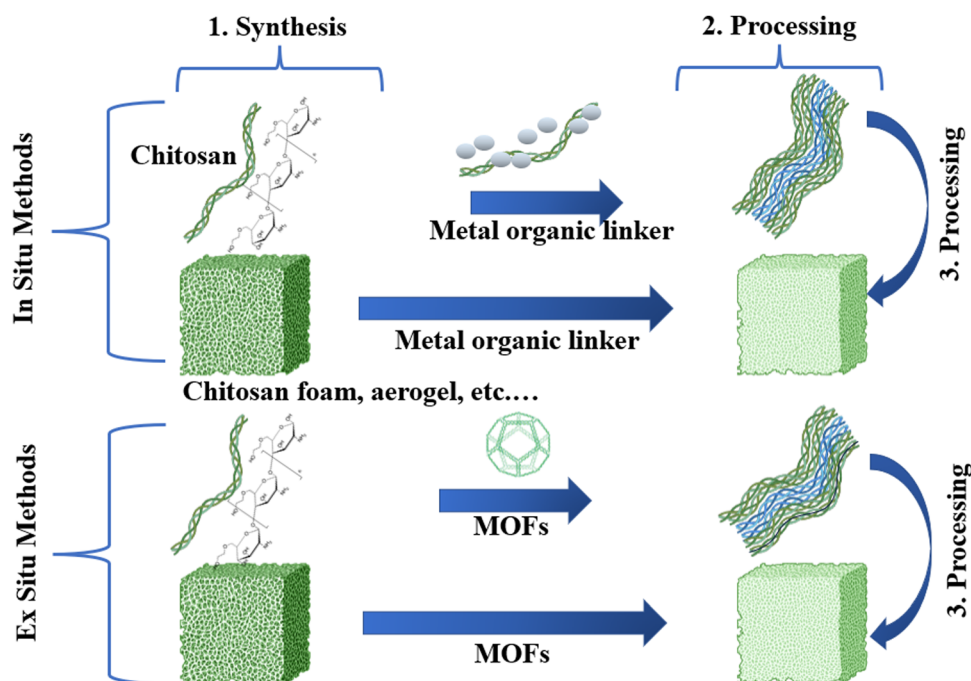 As these dyes resist bio-degradation, eliminating these noxious compounds is necessary for societal and environmental concerns.[90]

Saeed *et al.* (2022) discussed the preparation of CS/MOF-25 using the solvothermal method displaying an effective surface area of 30 m^2 g^{-1}. The adsorption experiments indicted an uptake capacity of 2857–2326 mg g^{-1} for CS/MOF-25, which is 14 times greater than CS, respectively. The hydrogen bonding, π–π bonding, pore-filling, electrostatic interaction and chemisorption were mainly responsible for the dye removal. The ethylene diamine functionalized ZIF-8 was incorporated into CS/PVA to form a membrane adsorbent to remove green 19. The membrane adsorbent was highly efficient in removing the dye, with a sorption capacity of 144.61 mg g^{-1}. The removal rate is ascribed to the electrostatic interaction of ZIF-8 with dye yielded through surface modification of ZIF-8.[91]

Zhang *et al.* (2022) described the synthesis of core–shell hybrid aerogel using both ionic cross-linking and a coordination bonding strategy.[92] A three-dimensional network of cellulose nanocrystals/carboxymethyl cellulose and MOF, respectively, form the core and shell of the generated aerogel beads.

Fig. 8 Different preparation strategies of CS/MOFs adopted for different applications.

The produced aerogel spheres have a methylene blue adsorption capacity of 1112.2 mg g^{-1}. The dye adsorption is mainly due to multilayer adsorption and follows the Freundlich isotherm model. Even after five cycles, only 20% reduction in adsorption capacity was observed.

Zhang *et al.* (2022) prepared different MOF-based adsorbents such as ZIF-8@attapulgite-CS, Zr-MOF@attapulgite-CS, and Al-MOF-@attapulgite-CS respectively. Both CS and attapulgite were added as supports to aid adsorption and enhance removal efficiency. Among these materials, Zr-MOF@attapulgite-CS illustrated a sorption capacity of 442.86 mg g^{-1} within 30 minutes of equilibrium time (methylene blue). This material also displayed reusability for up to five consecutive cycles without reducing removal efficiency. The system followed pseudo-second-order kinetics. The π–π interaction among the methylene blue and the organic ligand of Zr-MOF@attapulgite-CS is responsible for the degradation mechanism.[93]

Highly efficient CS/PVA/Uio-66/nanodiamond was developed *via* electrospinning for the destruction of Congo red (1430 mg g^{-1}). Rational design of adsorbent enhanced the efficacy of the nanofiber which is ascribed to electrostatic attraction and repulsion. The developed nanofiber composite is flexible, porous, and permeable. Higher reusability is the predominant advantage of electrospun nanofibers.[94] Chen *et al.* (2023) emphasized the fabrication of polyethyleneimine/CS/Ce-UIO-66 hydrogels *via* an *ex situ* blend method. The experimental studies indicated a maximum adsorptive elimination of methyl orange (900 mg g^{-1}). The electrostatic interaction of hydrogen bonding very much helped in the reclamation of methyl orange.[95]

5.1.2 Pharmaceuticals. There is a steady increase in the concentrations of pharmaceutical compounds found in the aquatic environments due to the huge consumption of pharmaceuticals and improper waste management.[80,96,97] Researchers also proved the existence of pharmaceuticals in different water matrices, for example, ground and surface water.[98,99] The elimination of pharmaceuticals is a prerequisite to safe water.[100,101]

The MIL-101 (Fe)/ZnO-CS composite beads were fabricated *via* ionotropic gelation. The morphological studies claimed octahedral geometry and uniform size distribution for MIL-101 (Fe). With the incorporation of CS, a uniform spherical structure with a rough surface is observed with a surface area of 8.38 m^2 g^{-1}. MIL-101(Fe)/ZnO-CS composite beads reported a sorption capacity of 31.12 mg g^{-1} toward tetracycline removal. The sorbent also exhibited a removal efficiency of 90% even after five consecutive cycles. The π–π interaction among the aromatic rings of tetracycline and adsorbent was the responsible mechanism for the degradation of tetracycline.[102] Yadav *et al.* (2022) emphasized preparing highly recyclable Fe$_3$O$_4$-functionalized MIL-101(Fe) CS beads using an ionotropic gelation method to eliminate antibiotics from water. The presence of CS is ascribed to the abundant number of active sites, adsorption, and flexibility of the beads. Scanning electron microscopy exhibited the greater adherence of the Fe$_3$O$_4$ particles on the rough surface of MIL-101(Fe). The sorption studies claimed a capacity of 45.33 mg g^{-1} for tetracycline. The bead
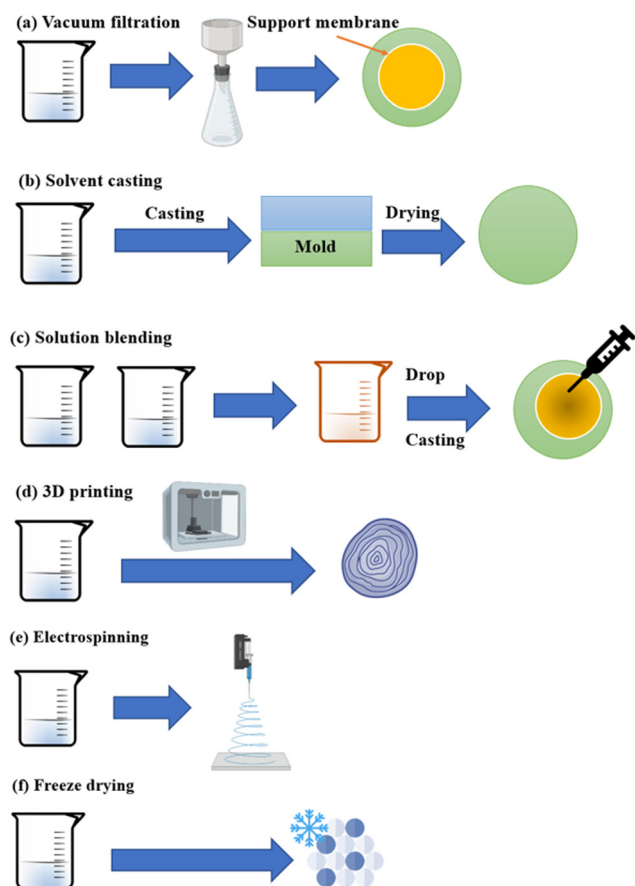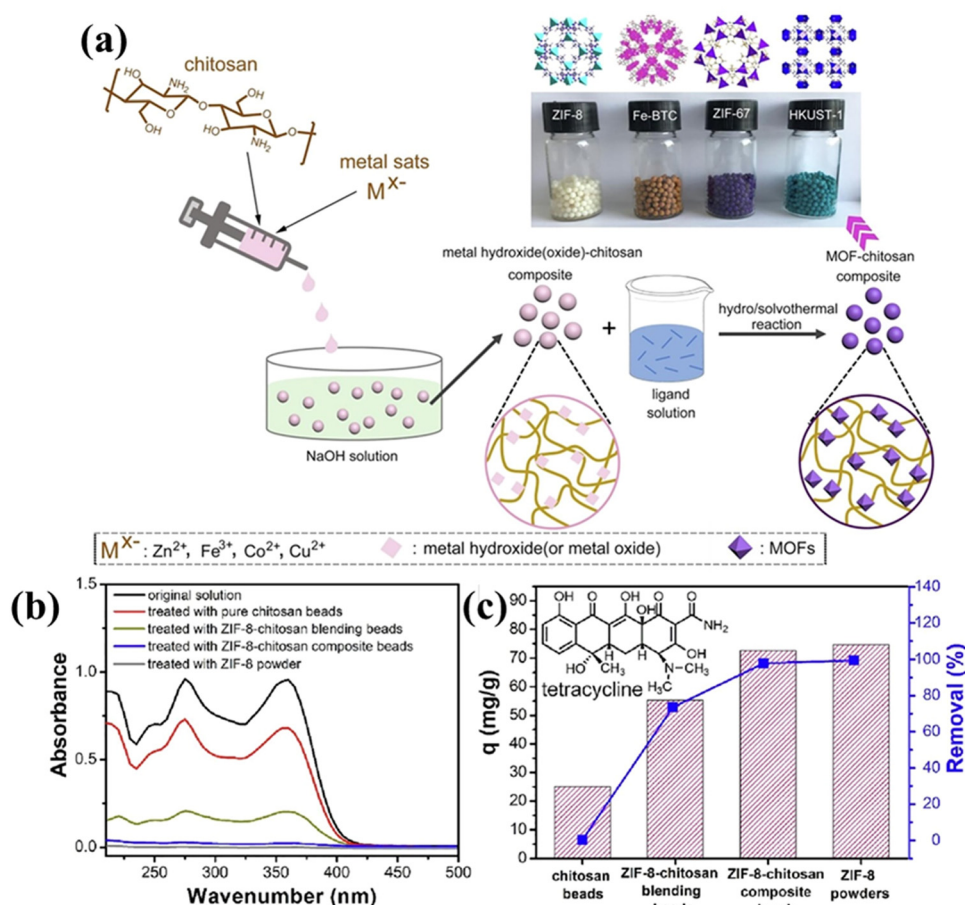
Fig. 9 (a) Diagrammatic representation of the CS/MOFs composite fabrication using the *in situ* growth method. (b) UV-vis spectra of tetracycline solution treated with different adsorbents. (c) Adsorption capability of the different adsorbents. Reproduced with permission.[105] Copyright 2020, Elsevier.

also displayed excellent reusability for up to five cycles. The major mechanism for removing antibiotics using beads is π–π interaction and hydrogen bonding with electrostatic interaction.[96]

In another study, the adsorptive removal of ketoprofen and ibuprofen using MIL-101(Cr)/CS beads was carried out. The prepared CS beads demonstrated a very incremented surface area of 800 m^2 g^{-1} compared with their pristine form (48 m^2 g^{-1}). Adsorption studies proved the viability of adsorbents in eliminating pharmaceuticals. The CS–MOF beads exhibited reusability for up to 7 cycles by maintaining the adsorption stability. The π–π interaction of aromatic groups between the adsorbent and pollutants is ascribed to the adsorption.[103] Jia *et al.* (2021) conveyed the immobilization of CS grafted carboxylic acid Zr-MOF onto porous starch using a facile CS adhesives strategy. The presence of porous starch offers a unique macro-porous structure skeleton to accommodate UiO-66-COOH particles. On the other hand, CS strengthens the electrostatic interaction and hydrogen bonding with the MOF and porous starch. The CS binding decreased the adsorbent's surface area to 52.4 m^2 g^{-1}. The modified CS displayed an adsorption capacity of 50.25 m^2 g^{-1} and reusability up to four cycles towards sulphanilamide.[104]

Later, Zhao *et al.* (2020) described the fabrication of MOF-incorporated CS beads for the reclamation of tetracycline. MOFs such as ZIF-8, ZIF-67, HKUST-1 and Fe-BTC were

incorporated to form a bead to avoid the problem of poor reusability and the high cost of catalyst separation. Fig. 9a illustrates the preparation of CS/MOF beads using the *in situ* growth method. The CS/metal oxide beads from the acid-dissolved/alkali-solidified self-sphering process were adopted as a substrate for immobilizing MOFs. The metal oxide acted as the base template for the growth of MOFs. Among these materials, CS/ZIF-8 composite beads demonstrated a higher adsorption capacity of 495 mg g^{-1} and retained 90% and above tetracycline removal efficiency even after a number of cycles (see Fig. 9b and c). Both of these studies targeted enhancing the reusability of the adsorbent.[105]

5.1.3 Heavy metals. The discharge of heavy metals from industries has tremendously increased during the past decades, alarming both man and animals.[106] Unlike other pollutants, heavy metals are not eliminated by microorganisms. As a result, they remain unchanged in the environment by increasing toxicity in soil, water, and the food chain. The heavy metals also cause severe health problems, including liver damage, skin disorders, damage to the nervous system, *etc.*[107] Eliminating heavy metals is a prerequisite to ensure manhood's safety.

Hu *et al.* (2022) described the CS-assisted MOF dispersion using covalent bonding interaction to eliminate heavy metals from wastewater. Here, a new strategy was proposed to
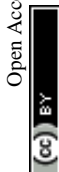
overcome the problems associated with serious agglomeration. UiO-66-NH$_2$ was chosen as the MOF material and grafted on CS via covalent interaction with the help of glutaraldehyde. The study reported that grafting MOFs onto the CS structure improved the MOF's dispersion and retained the MOF's morphology. However, incorporating CS reduced the surface area of UiO-66-NH$_2$ from 781.5 to 363.9 m^2 g^{-1} due to non-porous CS. The experiments reported a maximum sorption capacity of 364.96 and 555.56 mg g^{-1} for Cu(II) and Pb(II) within 45 minutes, respectively.[108]

Huang et al. (2022) emphasized the fabrication of MOF-derived Co–Al-LDH@CS/Fe$_3$O$_4$ for the elimination of Pb(II) and Cr(VI). The Pb(II) and Cr(II) sorption capacities are 558.84 and 710.79 mg g^{-1}, respectively. The adsorption kinetics proved that sorption occurred via chemisorption, and the rate-limiting step is exterior dispersion. The prepared adsorbent displayed better selectivity and reusability up to five cycles. The density functional theory proved the –SH and –NH$_2$ present on the surface of Co–Al-LDH@CS/Fe$_3$O$_4$ exhibited good affinity towards heavy metals. Chelation and electrostatic interaction was the responsible mechanism for heavy metal removal, which was proved via XPS analysis and zeta potential.[109]

Zhu et al. (2022) described the in situ growth of ZIF-8 on the carboxymethyl CS beads for the enhanced adsorption of Pb(II) ions present in wastewater. The sorption experiments reported a maximum adsorption capacity of 566.09 mg g^{-1} with reusability of 4 cycles. The studies proved the phenomenal role of NH$_2$ and COOH in the carboxymethyl CS in the chelation of lead ions.[110] Zaman et al. (2022) focused on the microwave-assisted preparation of CS-UiO-66-glycidyl methacrylate MOFs to remove Pb(II). The formulated sorbent indicated a phenomenal surface area of 867 m^2 g^{-1} with a thermal stability of 400 °C. The CS–MOFs retained 83.45% removal efficiency after 5 cycles.[111] Wang et al. (2023) stressed the development of magnetic MIL-125-NH$_2$/CS towards the reclamation of Cr(VI). The MIL-125-NH$_2$/CS demonstrated a maximum sorption capacity of 109.46 m^2 g^{-1} which is attributed to the uniform suspension of MIL-125-NH$_2$/CS in water, higher surface area and greater number of active sites.[112]

5.1.4 Other pollutants. Luo et al. (2019) studied the potential capability of Al-MOF/sodium alginate–CS beads to eliminate bisphenol A. The surface morphology confirmed that incorporating CS made the beads smoother and decreased surface-exposed nanoparticles. Both sodium alginate and the CS experienced strong encapsulation due to interactions between the alginate and the CS leading to the formation of denser beads. The hybrid beads exhibited a very high surface area of 687.5 m^2 g^{-1} and a micropore volume of 0.19 cm^3 g^{-1}. BET studies proved that CS was major in generating new micropores in the beads. The Al-MOF/sodium alginate–CS beads displayed a sorption capacity of 136.9 mg g^{-1} removal of bisphenol-A at a pH of 8 and 18 hours, respectively. The hydrogen bonding, π–π interaction, and cation–π bonding were major adsorption mechanisms for bisphenol remediation.[113]

Motaghi et al. (2022) reported that magnetic CS/activated carbon@UiO-66 usage for the ultrasound-assisted simultan-

eous adsorption of different noxious pollutants like Co(II), malachite green, and imidacloprid from aqueous streams. The adsorption studies claimed 44.5, 62.1, and 25.2 mg g^{-1} of adsorption capacity for Co(II), malachite green, and imidacloprid in the ternary system. The adsorptive process followed the PSO model, and thermodynamic studies indicate it is an endothermic process. Magnetic CS/activated carbon@UiO-66 is an environmentally friendly, cost-effective adsorbent with greater efficiency and reusability.[114] Le et al. (2023) utilized an in situ strategy for the successful development of Cu-MOF/CS beads. The developed Cu-MOF/CS beads reported a 120 m^2 g^{-1} adsorptive removal of toluene at 25 °C.[115]

Huang et al. (2020) emphasized the removal of 2,4-dichloro-phenoxyacetic acid using ionic liquid-modified CS/UiO-66. A BET study claimed that the ionic liquid-modified CS/UiO-66 exhibited a surface area of 204.33 m^2 g^{-1}. Experimental studies claimed that the adsorbent exhibited a sorption capacity of 265.25 mg g^{-1}. The better 2,4-dichlorophenoxyacetic acid removal is due to the increment in oxygen-containing groups, which promote the formation of hydrogen bonds in the adsorption.[116] Yang et al. (2021) developed nano ZIF-8@CS micro-spheres using inverse emulsion and in situ growth methods. The experimental studies reported a sorption capacity of 128.7 mg g^{-1} for removing p-hydroxybenzoic acid from the agro-industry. The ZIF-8@CS microspheres also exhibited a maximum of three consecutive cycles.[117]

Overall, CS/MOFs exhibit exceptional properties in removing different organic pollutants. The major advantages of CS/MOFs are the high porosity with multifunctional groups functioning as active adsorption and high stability attributed to forming highly stable complexes with centered metal ions in MOFs. Table 1 summarizes different CS/MOFs for the adsorptive reclamation of noxious pollutants. Despite its excellent adsorption capacity, CS/MOF beads suffer several problems like:

• CS demonstrated lower solubility in water, negatively affecting the fabrication of MOF composites. The alteration of CS to a water soluble form is very difficult.

• The CS/MOFs beads are also susceptible to biofouling, and organic fouling during the sorption of noxious pollutants.

• The selectivity of CS is yet another concern during the adsorption process. This issue can be resolved by utilizing molecular printed CS and MOFs.

• The stability and the reusability of the CS/MOFs must be explored in detail. Special focus must be given to synthesizing beads, aerogels, and nanofibers for their extended reusability. Along with that, adsorption experiments using real wastewater are highly desired to understand the feasibility of the adsorbent.

5.2. Removal of gases and particulate matters

The primary cause of global warming is the unchecked generation of carbon dioxide from various human activities.[138] In the past 150 years, carbon dioxide has increased from 250 to 418 ppm.[2] The higher concentration of carbon dioxide in the environment causes health risks to human beings and the environment.[139] The adsorptive-based carbon dioxide removal

Table 1 CS/MOFs for the adsorptive reclamation of noxious compounds

Adsorbent	Preparation route	Form	Metal core	Pollutant	Adsorption capacity (mg g^{-1})	Reusability	Mechanism	Ref.
ZIF-8 @CS poly vinyl alcohol	—	Nanofiber	Zn/Co	Malachite green	1000	—	Electrostatic interaction	118
CS/UiO-66	Impregnation	Composite	Zr	Methyl orange	370	4	Electrostatic interaction	54
HKUST-1 modified cellulose/CS composite	—	Aerogel	—	Methylene blue	526.3	5	Electrostatic attraction and hydrogen bonding	61
MIL-53/CS		Hydrogel	Fe	Congo red	590.8	3	Pore filling and ionic interaction	119
Citric acid cross-linked Zn-MOF/CS	Immobilization	Composite	Zn	Methyl orange	220	5	Electrostatic attraction and cation-π interaction	120
ZIF-8@CS sponge	*In situ* method	Sponge	Zn/Co	Congo red	987	5	Electrostatic attraction	121
MIL-101(Fe)@ CS	Immobilization	Sponge	Fe	Acid red 94	4518	3	Hydrogen bonding and coordinate interactions	122
CS/Fe$_3$O$_4$/MII-101(Cr)	—	Composite	Cr	Methyl orange	117	—	—	123
CS/UiO-66	Ice-templating	Monolith	Zr	Congo red	246	4	—	124
TIF-A!/CS	Secondary growth model	Beads	Al	Pb(II)	397.3	5	Chelation	125
ZIF-67 modified bacterial cellulose/CS composite	*In situ* method and lyophilisation	Aerogel	Co	Cu(II)	200.6	5	Electrostatic interaction	126
ZIF-67@ aminated CS beads	—	Beads	Co	Cr(VI)	119.05	7	—	127
CS-industrial hemp residue superfine powder-Fe@ZIF-67	—	Aerogel	Co	As(v)	22	—	—	128
CS-ZIF-8	*In situ* method	Beads	Zn/Co	Cu(II)	165	5	Ion exchange	129
				Pb(II)	131	5		
CS-*grafted*-poly(*N*-vinyl caprolactam)-ZIF-8	Electrospinning	Nanofibers	Zn/Co	Cr(VI)	269.2	5	Physical adsorption and π–π interaction	130
				As(v)	258.5	5		
MIL-100(Fe)/Fe$_2$O$_4$/CS	Grafting	Composite	Fe	Sb(III)	—	4	Surface complex binding of hydroxyl	131
ZIF-8@ CS microspheres	Inverse emulsion and *in situ* growth	Beads	Zn/Co	*p*-Hydroxybenzoic acid	128	3	Electrostatic interaction, hydrogen bonding	117
Porous starch CS-UiO-66-COOH	Facile CS-adhesive strategy	Composite	Zr	Sulfanilamide	—	4	Monolayer chemisorption	104
CS/ZIF-8 composite monolithic beads	—	Beads	Zn/Co	Uranium	629	4	Chelation	132
CS-UiO-66	Simple gelation and freeze casting	Beads	Zr	As(III)	47.9	5	Inner sphere complex	133
CS-graphene oxide/ZIF-8	*In situ* growth	Foam	Zn/Co	Uranium	361	5	Electrostatic interaction, intraparticle diffusion and coordination	134
MOF-808/CS	—	Composite	Zr	Cr(VI)	320	6	Hydrogen bonding and electrostatic interaction	135
Cu-MOF/alginate/CS/cellulose nanofibril composite	*In situ* growth	Hydrogel	Cu	Pb^{2+}	531.38	5	Ion exchange	136
CS/Uio-66-NH$_2$		Composites	Zr	Hg^{2+}	896.8	6	—	137

attained research importance due to its reversibility and versatility. For instance, Singo *et al.* (2017) also reported the preparation of CS-impregnated sodalite zeolite–metal MOFs to capture carbon dioxide. The adsorption studies were conducted in a packed bed reactor using 15% and 85% carbon dioxide and nitrogen, respectively. The impregnated CS/MOF displayed a maximum adsorption capacity of 978 mg g^{-1} at 25 °C.[140]

Jiamjirangkul *et al.* (2020) utilized MOF-integrated CS/PVA nanofibrous membrane hybrids to capture carbon dioxide. This study adopted three different strategies for the preparation of Cu-BTC/CS fibers hybrids *via* (i) direct mixing of Cu-BTC MOF with the CS/polyvinyl alcohol solution before electrospinning which was determined to be direct method, (ii) the formation of Cu-BTC MOF in CS nanofibers through an *in situ* method, and (iii) deposition of Cu-BTC MOF on CS nanofibre termed as the deposition method as highlighted in Fig. 10(I). Fig. 10(II) shows

a diagrammatic representation of the preparation of Cu-BTC/CS nanofibrous hybrids *via* deposition of Cu-BTC/CS nanofibrous membrane. The nanofibrous membrane was successfully prepared *via* layer-by-layer deposition of Cu^{2+} as a metal cluster and BTC as an organic precursor to form Cu-BTC MOF nanoparticles on the surface of the fiber. Studies also proved that the prepared material's surface area and pore size is altered by changing the order of precursor mixing. The prepared membrane exhibited 14 times higher carbon dioxide sorption capacity.[141]

In another study, CS/ZIF-8 beads were developed by the *in situ* growth method for carbon dioxide adsorption. The coordination of the free NH$_2$ group present in the CS skeleton with Zn^{2+} and self-emulsifying properties played a phenomenal role in the *in situ* growth of ZIF-8 on the CS beads. The CS-ZIF-8 beads exhibited 90% adsorption of carbon dioxide in compa-

rison with pristine ZIF-8. Carbon dioxide adsorption occurred *via* physical adsorption and exhibited more than 80% adsorption efficiency even after three consecutive cycles.[144]

Some researchers also tried other gases like formaldehyde. For example, Zhang *et al.* (2021) discussed the capability of CS cross-linked MOF-199@ aminated graphene oxide aerogel for the adsorptive removal of formaldehyde gas. The three-aerogel exhibited good thermal stability and reported a maximum sorption capacity of 197.89 mg g^{-1} of formaldehyde gas.[145]

Like carbon dioxide, air pollutants like particulate matter $(PM)_{2.5}$ cause significant health issues.[146] Air filtration is needed to overcome the exposure of particulate matter in our atmosphere.[142] Pan *et al.* (2021) reported a MOF-5/electrospun CS/polyethylene oxide membrane to remove $PM_{2.5}$. The CS/PEO@MOF-5 nanofiber membrane exhibited predominant $PM_{2.5}$ filtration efficiency and a quality factor of 99.95% and 0.0737.[147] A facile preparation strategy was proposed to efficiently integrate MOFs with cellulose paper and ZIF-8. The ZIF-8 was prepared *via* the *in situ* method in CS gel and followed by inclusion into the cellulose pulp to the composite design paper. The experimental studies reported 99.68% removal of $PM_{2.5}$ with a base weight of 60 g m^2. Fig. 10(III) emphasis the higher reusability of the CS/MOFs membrane with a PM2.5 removal efficiency of 96.46% at the 30th day with the increment

in pressure drop. The morphological analysis of the CS/PEO/MOF-5 membrane after the passage of polluted air affirmed the homogeneous capture of particulates on the surface of the membrane (Fig. 10(IV)(a) and (b)). In Fig. 10(IV)(c), the CS/PEO@MOF-5 membrane possessed two sides, one side indicates polluted air and the B side indicates filtered air. The change in colour from white to yellow is seen with the increase in the filter time for cell A affirming the higher capture of particulate contaminants and the colour on the B-side indicates minor variations.[142] Thus, the extraordinary structural integrity, durability and dust-holding capability of the modified membrane is claimed.

Hao *et al.* (2022) reported that MIL-125-NH$_2$ incorporated bacteria cellulose/CS foams were used as an efficient air filter to remove particulate matter. The directional freeze–drying approach successfully synthesized the foam matrix composed of mesopores or macropores of the polymer skeleton, yielding accessibility towards the MOFs and reducing gas diffusion barriers. Studies reported a maximum filtration efficiency of 99.5% with long-term stability of 30 days (see Fig. 10(V)). The electrostatic interaction between the CS/MOFs and particulate matter was the predominant filtration mechanism.[143]

Overall, the CS/MOFs were able to remove toxic gases and particulate matter from the environment. The CS/MOFs
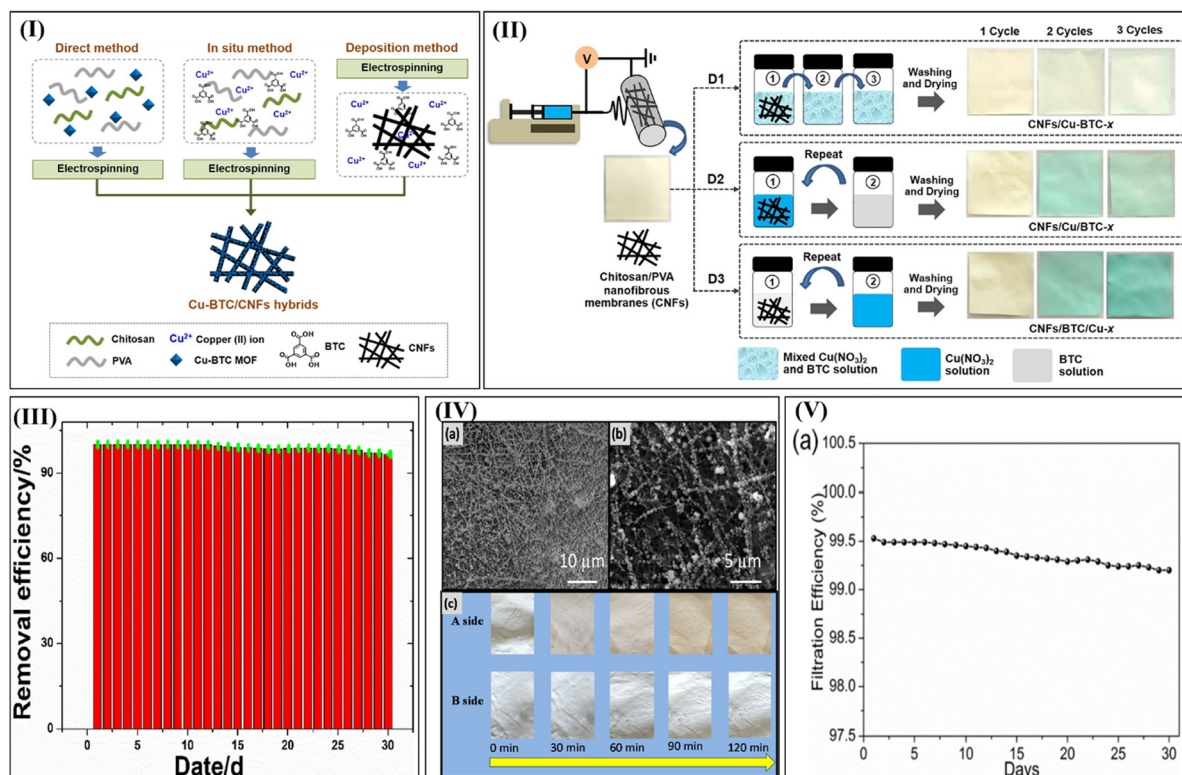
Fig. 10 (I) Schematic illustration of different preparation routes of Cu–BTC/CS nanofibrous hybrids, (II) diagrammatic representation of the fabrication route of Cu–BTC/CS nanofibrous hybrids *via* the deposition method. Reproduced with permission.[141] Copyright 2020, Elsevier. (III) Reusability of the CS/PEO@MOF-5 membrane towards the removal of $PM_{2.5}$, (IV) (a) SEM images of the CS/PEO@MOF-5 membrane treated with $PM_{2.5}$, (b) higher magnification version of the SEM image, and (c) photos of the CS/PEO@MOF-5 membrane under different PM capture. Reproduced with permission.[142] Copyright 2020, Elsevier. (V) Stability of MIL-125-NH$_2$ incorporated bacteria cellulose/CS foams. Reproduced with permission.[143] Copyright 2022, Elsevier.

exhibited good efficiency and stability. However, very limited studies were conducted using CS/MOFs. Continuing research is necessary to check the feasibility of CS MOFs against toxic gaseous pollutants. In addition, greater priority must be given to the beads, aerogels, hydrogels or membranes to ensure higher stability and reusability.

5.3 Catalytic applications

Photocatalysis is a highly utilized advanced oxidation process for wastewater treatment.[82,84,148] Photocatalysis attained research importance due to its high efficiency, environmental friendliness, no formation of by-products and complete mineralization of pollutants.[73] Very few researchers synthesized CS/MOF-based photocatalysts for environmental remediation. For example, an immobilized $Cu_3(btu)_2$-graphene oxide-CS hybrid photocatalyst was developed to remove methylene blue. The UV-diffuse reflectance spectra revealed a reduced band gap of 2.75 eV and an increment in the specific surface area to 947 $m^2 g^{-1}$. The photocatalytic degradation studies reported 98% methylene blue removal at a pH of 7 (time: 60 minute) using ultraviolet light.[149]

Vigneshwaran et al. (2022) emphasized the development of Fe_2O_3-supported micropillared Cu-BTC tethered over CS via the hydrothermal method. The MOF-based catalyst displayed 91% removal of paraquat within 60 minutes at a pH of 5. The hydroxyl radicals portrayed a major role in the reclamation of paraquat and followed pseudo-first-order kinetics. The CS/MOF displayed a maximum reusability up to 5 cycles. The improved reusability is ascribed to the magnetic behaviour of the photocatalyst (saturation magnetization of 9.565 emu g^{-1}). The studies also claimed that the tuned band gap and hindered recombination increased visible light activity.[150]

The $Zn_2(BDC)_2(DABCO)$-CS-Fe_3O_4 nanocomposites were prepared by Ghourchian et al. (2021). SEM analysis reported the homogeneous dispersion of magnetic CS particles on the MOFs without any aggregation. The saturation magnetization of the prepared photocatalyst declined from 66 to 36 emu g^{-1}. However, an increment in surface area is reported from 49.67 (MOF) to 148.83 $m^2 g^{-1}$ for the MOF-CS-Fe_3O_4. Experimental studies reported 99% removal of methyl orange within 23 minutes.[151] Novel AgO-CoO-CdO/poly-alanine-CS reduced graphene oxide (rGO) nanocomposites were reported using the sonication approach with a band gap of 1.51 eV. The photo-studies indicated a 97.4% methyl orange redemption. The better catalytic potential is ascribed to the incorporation of poly-alanine-CS-graphene oxide nanocomposites, which easily trap visible light photons and minimize the recombination ratio of e^--h^+.[152]

Vigneshwaran et al. (2021) has researched the preparation of MIL-88(Fe)-TiO_2-CS heterojunction via a solvothermal method. The composite removed 98.79% of monocrotophos within 30 minutes under visible light irradiation. The OH and $O_2^{\bullet-}$ radicals played a prominent role in the reclamation of pesticides. The photocatalyst also exhibited stability for five cycles. The prepared heterojunction consists of several high-speed nano tunnels in the p–n heterojunction facilitating the movement of photo-induced charge carriers and limiting electron recombination.[153]

From the limited number of studies, it is clear that CS MOFs can be used as an effective photocatalyst. The CS/MOFs photocatalysts can be recovered and reused for multiple cycles without too many complications (Fig. 11a). The main advantages of CS/MOF photocatalysts are illustrated in Fig. 11b. Despite their phenomenal efficiency, the following points need to be addressed.

● Extensive studies must be conducted on developing a low-cost synthesis route for CS/MOFs.

● Developing highly reusable photocatalytic beads via immobilization or using magnetic materials as support aids are highly required.

● No studies have been reported using solar light-driven CS/MOFs photocatalysis.
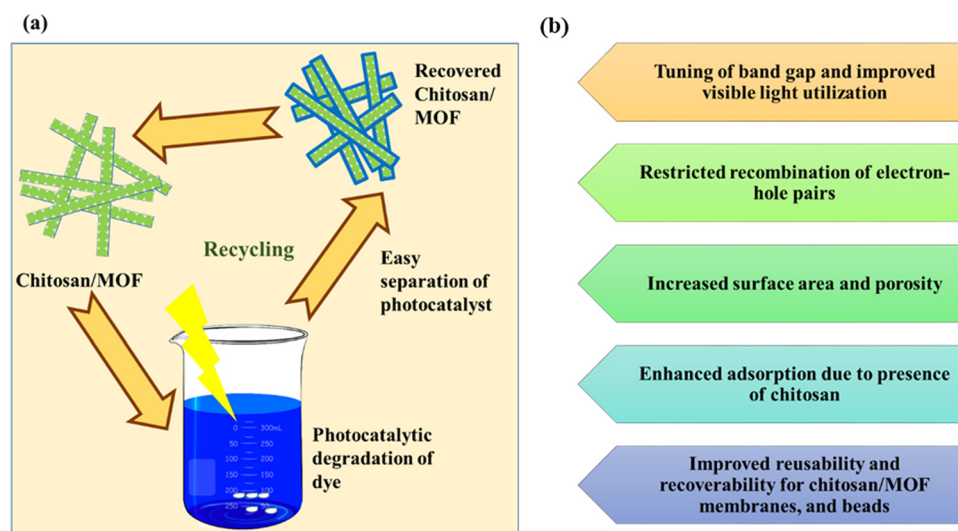

Fig. 11 (a) Pictorial representation of recycling CS/MOFs as a photocatalyst for the reclamation of dye wastewater under visible light. (b) The advantages of CS/MOFs as an efficient photocatalyst are also highlighted.

• Further studies are necessary to develop highly compact, cost and energy-efficient photocatalytic processes to enhance the catalytic activity to a greater extent.

A tandem reaction is an important reaction in which bonds are developed without isolating the intermediates, altering the reaction conditions or through inclusion of chemical reagents. Tandem reactions yield promising research attractions due to their simplicity and efficient utilization of atoms. Tandem reactions do not need any purification and separation of intermediate by-products. Zhao *et al.* (2020) explained the fabrication of CS-coated MIL-101(Cr) as effective catalysts for the tandem deacetalization-Knoevenagel condensation reaction. The CS-coated MIL-101(Cr) was fabricated *via* an *in situ* growth method, yielding good chemical and thermal stability and reusability. The CS coated MIL-101(Cr) exhibited a core (MIL-101(Cr))-shell structure (CS). Here MIL-101(Cr) possesses Lewis acidic sites, and CS provided both Brønsted acidic sites and Lewis basic sites. The synergistic effect between CS and MIL-101(Cr) offered a prominent catalytic activity toward the condensation reaction. The prepared catalyst also exhibited good reusability over five cycles.[154]

Yousefian *et al.* (2020) stressed the fabrication of Cu-MOF immobilized modified CS *via* combinations of terephthalic acid as an organic linker and Cu^{2+} as the metal constituent. The studies reported the Knoevenagel condensation reaction and the synthesis of benzylidene malononitrile under Cu-MOF/CS as an effective heterogeneous catalyst. The Knoevenagel products attained high yields under mild conditions and minimum time requirements. The catalyst is highly stable and exhibited high recovery for preparing benzylidene malononitrile

derivatives. The catalyst is reused eight times without a reduction in the efficiency of the catalyst.[155]

Wang *et al.* (2022) stressed the growth of MOF on CS as an effective host for palladium as a catalyst for Suzuki reactions. The ZIF-8 has been planted on CS microspheres using poly-dopamine as the base substrate. The preparation of CS/PDA@-ZIF-8@Pd by employing CS spheres as base templates to grow MOFs as core–shell microspheres with the phenomenal surface area is shown in Fig. 12a. The CS/PDA@ZIF-8@Pd exhibited K_{app} of 0.0426 s^{-1} for the reduction of *p*-nitrophenol. Fig. 12b represents the proposed mechanisms of the Suzuki coupling reaction using CS/PDA@ZIF-8$_{25}$@Pd. The ZIF-8 shells attached to CS microspheres *via* dopamine can fix Pd ions grown in its pores and restricts the size of Pd nanoparticles which provide a large number of active sites than larger Pd nanoparticles for quick electron transfer from an electron donor substrate to an acceptor to catalyze the p-NP and C–C coupling reaction. The unique core–shell structure possessing a surface area of 353.1 m^2 g^{-1} was responsible for the unusual catalytic activity. The prepared catalyst demonstrated a reusability of 6 cycles with a final yield of 94% for CS/PDA@ZIF-8$_{25}$@Pd which is highlighted in Fig. 12c. The minor decline in yield of the catalyst is ascribed to the agglomeration of the catalyst and the presence of inorganic ions on the material surface.[156]

5.4 Membrane separation

The mixed matrix membrane yielded from CS and MOFs are highly popular in separation technology. The better performance is ascribed to the special features offered by MOFs. The high

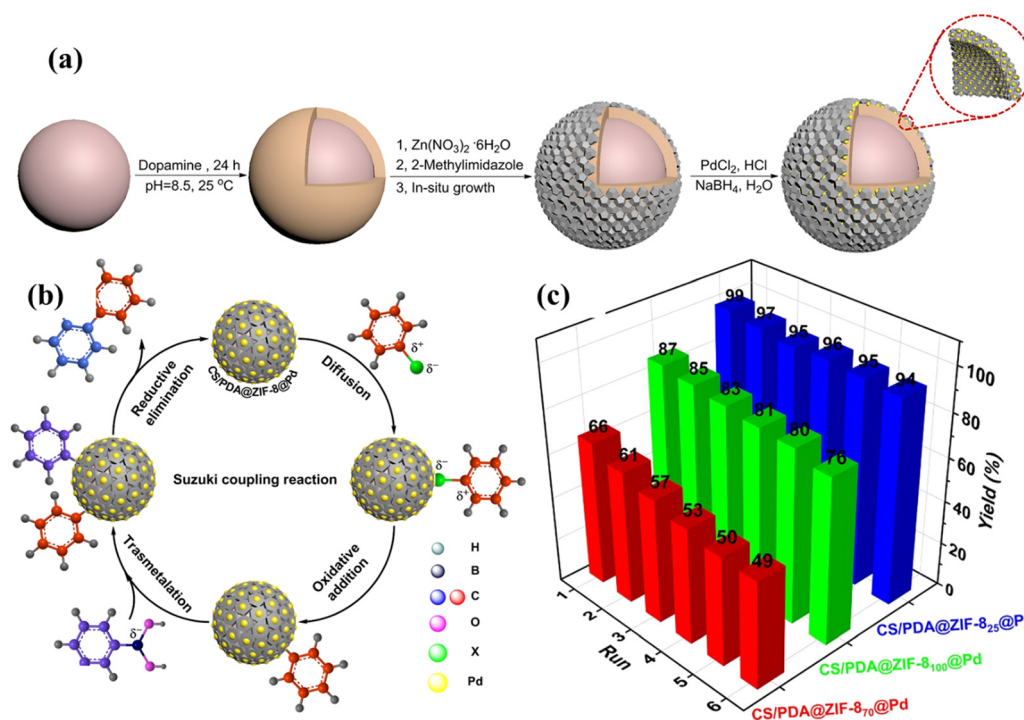
Fig. 12 (a) Preparation route of CS/PDA@ZIF-8@Pd microspheres by employing CS spheres as the base template to grow MOFs as core−shell microspheres with a phenomenal surface area, (b) proposed mechanism of the Suzuki coupling reaction using CS/PDA@ZIF-8@Pd as the catalyst, and (c) reusability of different catalysts for Suzuki reactions. Reproduced with permission.[156] Copyright 2022, Elsevier.

porosity, crystallinity, and surface area are important properties affecting the membrane's performance. Due to their improved mechanical properties, the CS/MOFs membrane exhibits high selectivity and withstands aggressive chemical environments. As a result, researchers are working in this field to enhance its potential applications.

Ma et al. (2017) developed a facile method for preparing a positively charged nanofiltration membrane. The membrane is prepared by blending both MOFs into the CS matrix for enhanced removal of cations. The MOFs, such as NH_2-MIL-101(Al) and NH_2-MIL-101(Cr), were uniformly dispersed in the CS matrix. Studies proved that the morphology of MOFs influenced the permeability of the membrane. The nanofiltration membrane of MOFs exhibited rod-shaped morphology and attained two times more flux. The rejection ratio of the nanofiltration membrane is found to be 93%.[157] Wang et al. (2022) described the fabrication of sulfonated polyether sulfone/N-phthaloyl CS/MIL-101(Fe) as a novel mixed matrix cation exchange membrane. The presence of MIL-101(Fe) improved the ion-selective separation by forming a hydrogen bond with the CS matrix of the membrane. The desalination rate of the membrane improved by 136%, while the energy consumption was reduced to 90%.[158]

Shi et al. (2021) prepared a UiO-66/tannic acid/CS/polyethersulfone hybrid membrane to remove dyes and Cr(vi). The prepared material was dense enough to perform filtration experiments like a membrane to eliminate cationic and anionic dye from water. About 99% filtration efficiency achieved within 200 minutes is ascribed to the dynamic filtration ability created via an improved driving force that occurred via concentration polarization. Studies also claimed that the MOF was core in dispersing the tannic acid-CS mixture to enhance pollutant removal.[159]

Lakra et al. (2021) described the development of a cellulose acetate-CS–MOF forward osmosis membrane to recover water and nutrients. The forward osmosis is prepared by coating a CS AlFu-MOF mix on a cellulose acetate membrane. The AlFu-MOF membrane separation improved hydrophilicity and resulted in greater water flux. Experimental studies reported 80% water recovery in forward osmosis and 85% salt rejection from dilute draw solution using reverse osmosis. The nutrients in the concentrated feed wastewater are recovered as struvite by precipitating the reject water of reverse osmosis.[160]

Pervaporation is a highly economical method for separating azeotrope mixtures, recovering heat-sensitive compounds, and eliminating low-concentrated noxious compounds from the aqueous streams. Xu et al. (2022) reported the capability of the CS/ZIF-8 mixed matrix membrane to effectively separate methanol/dimethyl carbonate. Experimental studies reported that the 15 wt% CS/ZIF-8 membrane exhibited outstanding selectivity of 11.2 and MeOH performance of 97.7 GPU at 50 °C. The excellent efficacy is ascribed to the greater affinity of MeOH towards CS.[161]

Zhu et al. (2022) described the effective separation of methanol/dimethyl carbonate using the UiO-66 MOF/CS membrane. The studies emphasized that UiO-66 fillers improved the CS membrane's permeance and selectivity. A total flux of 355 g m^{-2} h^{-1} and a separation factor of 337 were achieved, almost 25 times greater than the pure CS membrane.[162] Vinu et al. (2018) synthesized the microporous Al-MOF (Al(OH)(MBA)) using the hydrothermal and solvothermal methods. The MOFs were incorporated with the CS to form a mixed matrix membrane. The prepared MOF membrane effectively separated the water/ethanol mixture through pervaporation.[163]

The MOF (ZIF-8 or HKUST-1)/ionic liquid/CS mixed matrix membrane was successfully prepared to separate carbon dioxide/nitrogen. The presence of MOFs improved the selectivity of ionic liquid CS hybrid continuous polymer matrix. The experimental studies reported the permeability of the CO_2/N_2 selectivity performance is yielded for 10 wt% ZIF-8, and 5 wt% HKUST-1/ionic liquid CS membrane was 5413 Barrer and 11.5 and 4752 and 19.3 respectively. This is indicated by the better adhesion properties.[164]

Zhu et al. (2021) emphasized the preparation of the UiO-66-NH_2 CS composite membranes for oil–water separation. The prepared membrane demonstrated high hydrophilicity in the air and super-oleophobic performance underwater. During the separation of petroleum ether water emulsion, the filtration flux is reported to be 2000 L m^{-2} h^{-1}, and the filtration efficiency is greater than 95%. Even after ten cycles flux of

Table 2 Different applications of CS/MOF membranes in environmental remediation in an aqueous matrix

Analyte	Membrane	MOF	Separation mechanism	Observations	Ref.
Ethanol	CS	MOF-801	Pervaporation	Flux = 1937 g m^{-2}	167
Isopropanol	CS	ZIF-8	Pervaporation	Flux = 410 g m^{-2} h	168
Ethanol	CS	ZIF-7	Pervaporation	Flux = 322 g m^{-2} h	169
Methanol	CS	MIL-53	Pervaporation	Flux= 2329 g m^{-2} h^{-1}	170
Nitric oxide	CS	Cu-BTTri	Filtration	—	171
BSA protein	Polyvinylidene fluoride/CS	UiO-66-NH_2 ZIF-8	Ultrafiltration	Flux = 470 L m^{-2} h	172
				Rejection = 98.1%	
Cr(vi)				Rejection= 95.6%	
Pb(ii)	Polyvinyl alcohol/CS	UiO-66-NH_2	Filtration	Flux = 452 L m^{-2} h^{-1}	173
				Removal = 94%	
Cd(ii)				Flux = 463 L m^{-2} h^{-1}	
				Removal = 89%	
Cr(vi)				Flux = 479 L m^{-2} h^{-1}	
				Removal = 85.5%	

the membrane was very high, four times greater than the mixed cellulose membrane.[165] Si *et al.* (2023) focused on the separation of oil/water using ZIF-8@cellulose nanofiber/chitosan aerogel developed using a freeze-drying strategy. The predominant advantages of aerogels are higher porosity, light-weight and low density. The aerogel could easily separate oil from mixtures with assistance of gravity and displayed a reusability of 20 cycles.[166]

The CS/MOFs membranes are diverse materials exhibiting different applications in the allied areas of environment, separation and energy. Table 2 summarizes the different CS/MOF-based membranes for environmental remediation. Some of the challenges exhibited by CS/MOFs are.

• The pre-synthesis of MOFs particles are highly necessary to ensure the removal of residual foreign molecules. The MOFs under vacuum may destroy pores and affect the sieving effect upon doping into the membrane matrix. The stronger pressure may also decrease the porosity. Activating the pore structure of MOFs using lower surface tension solvents is beneficial.

• The requirement of high temperature and organic solvents is necessary for the research of CS/MOFs. The preparation of MOFs at a higher temperature may cause secondary pollution to nature by forming toxic by-products and consuming organic solvents. It is always desirable to develop greener pathways for developing CS/MOFs.

• The majority of researchers emphasized the separation of pollutants *via* size exclusion selectivity. However, it is not easy to employ size-exclusion during the separation of molecules with more similar sizes and polarizability.

• The biopolymer-supported MOFs are highly prone to fouling, impacting the permeate quality and reducing the flux. The surface engineering of CS/MOFs may overcome this issue.

5.5 Energy storage devices

Ever-increasing energy demands and the continuous shortage of fossil fuels have compelled us to explore renewable energy resources. The challenge with energy storage devices must be addressed to exploit renewable energy sources.[174] The need for sustainable elevated performance electrochemical energy storage and conversion devices is an emergency. The renewability, mechanical stability, flexibility, and durability makes the CS/MOFs suitable in different electrochemical energy storage and conversion devices such as supper capacitors, batteries and fuel cells.

Super capacitors are electrochemical energy storage devices that received the most research interest owing to their high power density, fast charging, and good cycle life.[175] Novel electrode and electrolyte materials need to be developed to enhance the stability and durability of supercapacitors. Ehsani *et al.* (2020) reported the preparation of ternary poly-*ortho* aminophenol (POAP)/CS/MOF-1 using the electropolymerization method as an effective electrode in a pseudo-capacitor. Here, $[Zn_2(bdc)_2(dbco)]_n$ is used as a MOF in this study and was prepared *via* simple chemical routes with a surface area of 124.18 m^2 g^{-1} for the ternary composite. The specific capacitance of the POAP/CS/DMOF-1 electrode is 3150 mF cm^{-2} at an optimum current density of 1 mA cm^{-2}. The predominant capacitive activity is indicated by the synergistic effect of the CS/DMOF-1. The Faradaic contribution of the DMOF-1 enhanced the electrochemical performance of the electrode. The device retained 93% of its initial capacitance over 1000 cycles at 10 mA cm^{-2}. The key merits of this composite electrode are higher active surface area, stability and easiness during the preparation.[176]

The hierarchically porous carbon derived from MOF/CS composites was used for the high-performance supercapacitor. A facile method was adopted for synthesizing porous carbon by calcinating MOF/CS composites. Studies claimed the prepared composite displayed a surface area of 2375 m^2 g^{-1} and a pore volume of 2.49 cm^3 g^{-1}. The electrode exhibited a better specific capacitance of 199 F g^{-1} in 1 M H_2SO_4 electrolyte and a good rate capability of 75% from 0.05 to 4 A g^{-1}. The supreme activity of the electrode is ascribed to the high surface area, pore volume, and the porous structure.[177] Recently a team of researchers demonstrated the effective mechano-chemical route for the fabrication of ZIF-8 nanocrystals and ZIF-8@CS for battery applications. A novel lithium-ion battery anode material was developed by pyrolyzing the ZIF-8@CS nanocomposites. The material exhibits a high specific capacitance, lower impedance, and greater stability.[178]

A ZIF-8-derived porous carbon supported on carbon aerogel derived from CS was recently developed using the facile *in situ* deposition method followed by carbonization. Fig. 13(i) confirmed the deposition of ZIF-8 polyhedron on the CS aerogel through the co-precipitation followed by calcination. Fig. 13(ii) compares the carbon aerogel with the CS aerogel obtained at the end of the carbonation process resulting from the pyrolysis of CS. The prepared aerogel is also found to be lightweight and capable of standing on a flower petal. The stacked layer-by-layer three-dimensional porous structure is exhibited by carbon aerogels with interlaced nanosheets (Fig. 13(ii)(c)). The structural analysis also proved that the carbon aerogels boost-up the electron and ion transport and can be utilized as a base skeleton for the growth of ZIF-8 possessing a polyhedral structure. The prepared ZIF-8 exhibited an average particle size of 0.5 μm (Fig. 13(iii)(a)) and the corresponding SEM image in Fig. 13(iii)(b). Fig. 13(iii)(c) and (d) depict the SEM and TEM images of ZIF-8-C, which affirms the polyhedral shape after converting ZIF-8 to ZIF-8-C, respectively. The ZIF-8-C is uniformly supported and well-distributed on the nanosheets of carbon aerogels to restrict the aggregation of ZIF-8-C as observed in Fig. 13(iii)(e). The TEM image of the ZIF-8-derived porous carbon reinforced on carbon aerogel derived from CS affirms the uniform deposition of ultrafine nanocrystalline powder on the carbon sheets (Fig. 13(iii)(g)). The results also indicated the development of homogenously supported ZIF-8-C on the three-dimensional carbon aerogel nanosheets. Fig. 13(iii)(f) and (h) show the occurrence of nitrogen and carbon. The presence of nitrogen functional groups incremented the pseudo-capacitance in the charging–discharging process. The prepared material exhibited a three-dimensional mesoporous structure with interlaced nanosheets acting as a
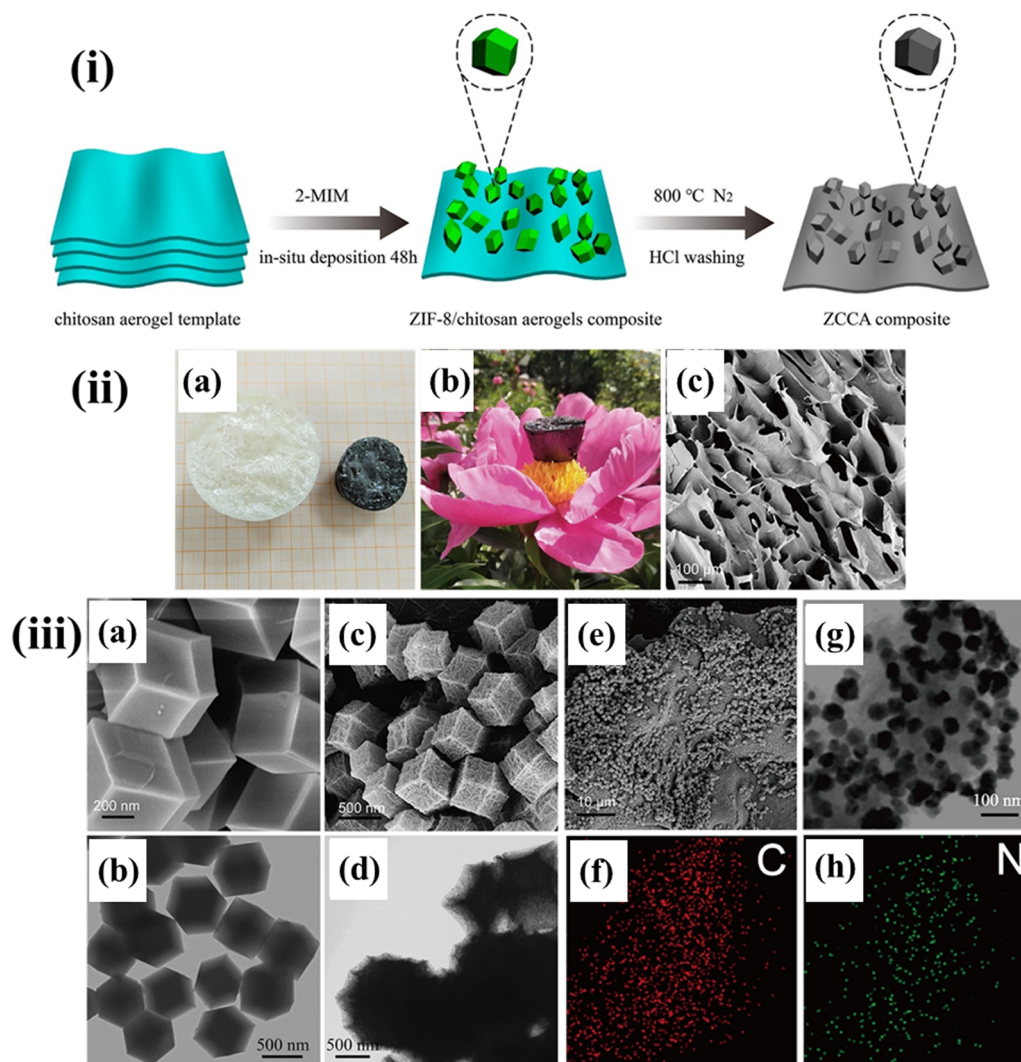
Fig. 13 (i) Schematic illustration of the formation of ZIF-8-carbon supported on carbon aerogel derived from CS. (ii) (a) A photograph of CS aerogel and carbon aerogel, (b) light-weight carbon aerogel on a flower, and (c) SEM images of the carbon aerogel. (iii) SEM images of (a) ZIF-8 and (b) ZIF-8-C, TEM images of (c) ZIF-8 and (d) ZIF-8-C, (e) SEM images of ZIF-8-carbon supported on carbon aerogel, (f) elemental mapping of carbon, (g) TEM images of ZIF-8-carbon supported on carbon aerogel, and (h) elemental mapping of nitrogen. Reproduced with permission.[179] Copyright 2020, Elsevier.

skeleton to grow ZIF-8-derived carbon. The presence of both mesopores and micropores creates more channels for electrolyte ions and provides electrical double-layer capacitance. Electrochemical performances revealed that the composite electrode exhibited a specific capacitance of 241.6 F g^{-1} at a current density of 0.5 A g^{-1} and retained a capacitance retention of 90% after 5000 cycles. The superior capacitive behaviour of the composite is indicated by the greater porosity of the continuous 3D structure which accelerated the electron/ion transport.[179]

The CS/MOFs are not well explored as a material for supercapacitors and batteries. Even though the results are good, further enhancement of the performance of the supercapacitor is necessary. The following parameters may require immediate attention to strengthen the efficacy of CS/MOFs as a supercapacitor or battery material. The fundamental mechanism behind the energy storage must be explored for interfacial

reactions at the electrode. In addition, adequate control of interfacial interactions is important to attain a high electrochemical efficiency. To develop a full CS/MOFs-based supercapacitor, CS-based electrodes should be assembled with CS/MOFs electrolytes in a single device, and the performance must be evaluated.

Fuel cells are energy conversion devices that are capable of generating electricity *via* an electrochemical reaction using a fuel and oxidant. Recently, Kumar *et al.* (2022) stressed the fabrication of sulfonated CS and copper-based MOF (HKUST-1) based membranes using the solution casting technique for direct methanol fuel cell applications. The surface morphology proved the incorporation of HKUST-1 as a pore-filling agent and the creation of finger-like hydrophilic channels into the sulfonated CS matrix. The intermolecular hydrogen bonding between the carboxylic group of HKUST-1 and SO$_3$H groups of sulfonated CS improves the performance in terms of ion
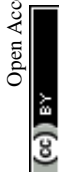
exchange capacity, thermal stability, and proton conductivity. The prepared membrane possessed greater proton conductivities of 5.38×10^{-3} and 6.19×10^{-3} S cm^{-1} at 25 and 80 °C respectively. However, because of its small ionic size, the sulfonated CS membrane exhibited lower methanol permeability and selectivity than the pristine sulfonated CS and commercial membrane. The phenomenal pore reduction ability of HKUST-1 allowed proton and blocked methanol permeation in the membrane matrix.[180]

In another study, a highly efficient proton exchange membrane SO$_3$H-UiO-66 coated halloysite nanotube-modified CS was formulated using a one-pot *in situ* growth method. Later it was used as an additive in the CS matrix to prepare the proton exchange membrane. The prepared membrane displayed strong mechanical strength and methanol resistance. The core–shell nanohybrids consist of 1-D halloysites nanotubes and MOFs with rich functional groups that enhance the water absorption characteristics. The core–shell nanohybrids eventually led to the development of interconnected water networks for speed proton transfer. As a result, the composite membrane displayed a conductivity of 46.2 mS cm^{-1} and a maximum power density of 84.5 mW cm^{-2}.[181] Further research is necessary to understand the capability of the CS/MOF.

5.6 Sensor applications

CS-based MOFs are a highly interesting material for sensing applications due to their gel-forming ability, hydrophilicity, better permeability, mechanical strength, and ease of employing reactive functional groups.

Choi *et al.* (2020) developed a co-hemin MOF/CS biosensor to detect lactose. The biosensor Co-hemin MOF was fabricated using the self-assembly of CoCl$_2$ with an organic linker. Here, Co-hemin MOF acted as a mediator for the development of biosensors. The Co-hemin MOF was later adsorbed on a glassy carbon electrode through the electrodeposition method. Experimental studies reported that the prepared MOFs displayed phenomenal electrochemical performance in detecting lactose with a greater high sensitivity of 102.3 µA mM^{-1} (time = 5 s) and a lower detection limit of 4 mM.[182] The biosensor also reported lactose in milk (46 g L^{-1}), goat's milk (42.76 g L^{-1}), drinking yogurt (5.99 g L^{-1}) and chocolate milk (12.44 g L^{-1}), respectively.

Huang *et al.* (2020) emphasized the development of CS/thiol functionalized MOFs for the detection of lead and cadmium ions in food samples. Under the optimized conditions, the detection limits of lead and cadmium ions were 0.33 and 0.008 µg L^{-1}. The results of method validation offer excellent selectivity, high sensitivity and simple operation. The authors also validated the presence of lead and cadmium ions in three different certified reference materials (CRM) such as rice, wheat and tea. For example, the detected value of lead and cadmium are 0.021 µg g^{-1}, 7 ng g^{-1}, 0.059 µg g^{-1} and 15 ng L^{-1} for wheat and 1.6 µg g^{-1} and 64 ng L^{-1} for tea, respectively. The certified and the reported values were found to be in agreement with each other. Because the highly rich and accessible –SH functional groups of the CS/MOFs may accelerate the detection of lead and cadmium ions.[183]

Miao *et al.* (2022) emphasized the preparation of CDs@ZIF-8/CS as a portable, disposable test strip. Fig. 14(I) describes the CDs@ZIF-8/CS dual-function thin-film sensor assembly. The sensing material was developed by encapsulating luminescent porous composites and incorporating CS into it. The CS
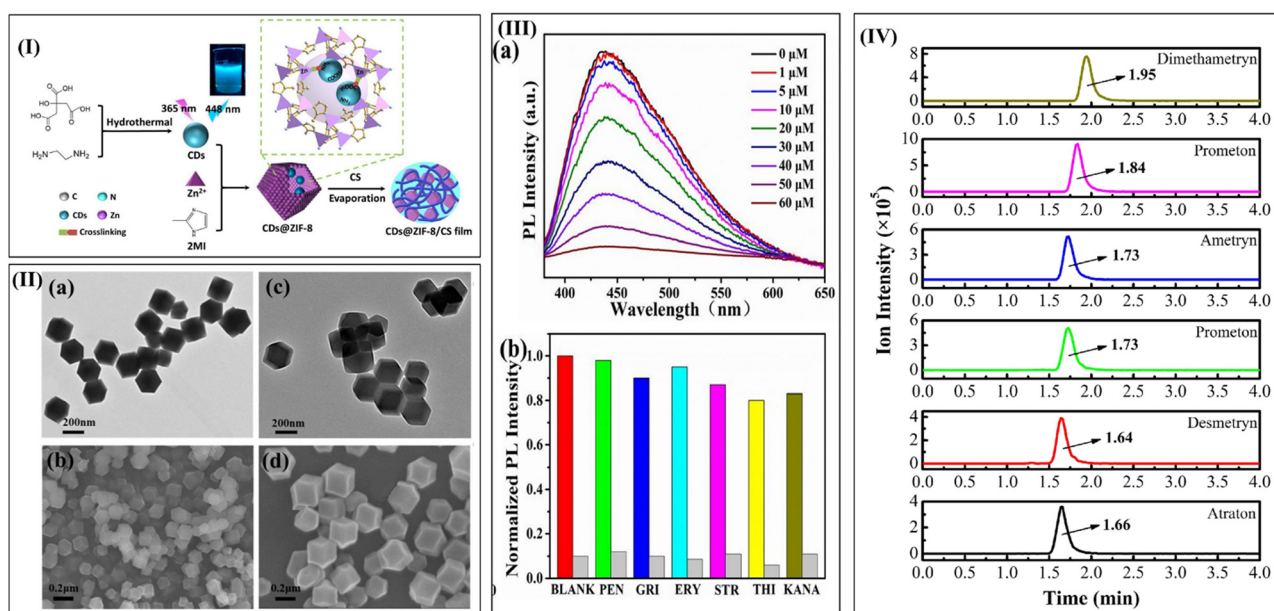
Fig. 14 (I) Schematic preparation of the CDs@ZIF-8 CS dual function thin-film sensor (II) (a) TEM image of ZIF-8, (b) SEM image of ZIF-8, (c) TEM image of CDs@ZIF-8, and (d) SEM image of CDs@ZIF-8. (III) Performance for detection, selectivity, and adsorption of CDs@ZIF-8/CS film for tetracycline: (a) fluorescence quenching, and (b) selectivity of CS/MOF to tetracycline. Reproduced with permission.[184] Copyright 2022, Elsevier. (IV) HPLC-MS/MS chromatograph of the different samples. Reproduced with permission.[185] Copyright 2021, Elsevier.

was an appropriate support to reduce the constraints related to secondary pollution impacted by powder composites. Along with this, the desired shape was also achieved. The formation of the CDs@ZIF-8 was indicated by the effective coordinate interaction between the Zn^{2+} and N-containing groups on the CDs surface during the ZIF-8 growth. The highly uniform sodalite zeolitic structure of ZIF-8 possesses a hexagonal shape with a size of 200 nm (Fig. 14(II)(a)–(d)). The introduction of the ZIF-8 to the CDs@ZIF-8 did not alter the morphology of ZIF-8. The film exhibited better sensitivity and selectivity for detecting tetracycline using a concentration quenching mechanism with a maximum detection limit of 0.60 μm (Fig. 14(III)).[184]

The preparation of the MIL-101(Cr)/CS functionalized hydrophilic sponge column with the help of a simple infiltration method was reported. The CS minimized the problem of adsorption and hydrophobicity. The role of CS was to act as both adhesives during the functionalization of an adsorption adjuvant in detecting herbicides. The formulated material was used as an adsorbent in a vortex-assisted slid-phase extraction. It was combined with HPLC tandem MS to determine six triazines in water samples such as prometryn, desmetryn, atraton, ametryn, prometon, and dimethametryn as shown in Fig. 14(IV). The proposed method could determine these compounds in five real water samples. The triazine herbicide detection limit in spiked water samples ranges from 0.014 to 0.045 ng mL^{-1}.[185] The key highlights of this study include simplicity, higher sensitivity, and minimum requirements of organic pollutants.

Si *et al.* (2022) specifically focused on preparing MIL-53(Al)/CS/polyethylene oxide composite columnar foam to determine estrogen in an aqueous solution. Here, polyethylene oxide was used to serve as a porogen to enhance the MOF loading capacity of the prepared foam. The lower limit of estrogen detection is 0.3 to 6.6 ng L^{-1}.[186] Due to outstanding characteristics like surface area and porosity, they were suitable for detecting different pollutants and compounds. The synergistic effect of CS and MOF leads to enhanced efficiency in sensing heavy metals and pharmaceutical compounds.

5.7 Packaging

Food wastage is a predominant concern for a sustainable society.[187] Active food packaging strategies can be adopted to reduce food waste, including incorporating active components into the packaging materials.[28] Packaging can overcome the problems of traditional preservation methods like freeze–drying, microwave and fermentation as they cause a difference in the quality and taste of food.[188] So, the CS/MOFs can be used as an active agent to increase shelf life and to ensure human health. The active agent, CS/MOFs packing, can be conducted *via* coating, sachets and an impregnation method, as shown in Fig. 15. However, a limited number of papers on CS/MOFs for food packaging are available.

The Ag@MOF-loded *p*-coumaric acid-modified CS/CS nanoparticle/PVA-starch bilayer film is used for food packing film. The novel bilayer film comprises two layers (i) Ag–MOF-*p*-coumaric acid-modified CS and (ii) PVA/starch as the top and
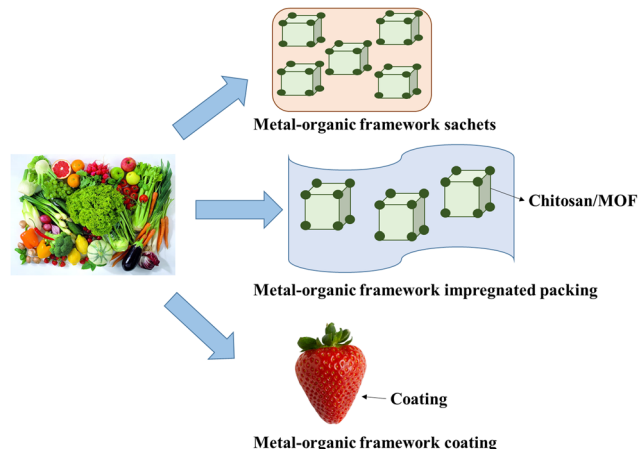

Fig. 15 CS/MOFs used in food packaging to preserve the food quality. Three methods for food packaging are adopted using MOFs: sachets, coatings, and impregnated packing.

bottom layers, respectively. The bilayer film displayed good oil resistance, antioxidant activity, cytotoxicity and optical properties. The film exhibited outstanding antibacterial activity against *E. Coli* and *S. aureus*. The surface of the bilayer film was highly smooth and exhibited a tensile stress of 27 MPa. The good UV-blocking properties, transparency, and ability to prevent bacterial infections make this film suitable for food industries.[15]

Kohsari *et al.* (2016) developed electrospun CS–polyethylene oxide nanocomposites composed of ZIF-8 using an electrospinning method. Studies reported that the CS-PEO-3%-ZIF-8 NPs could be highly adaptable for edible food coating due to its enhanced hydrophilic behaviour. The scanning electron microscopy affirmed the spherical ZIF-8 nanoparticles of 60 nm and the nanofibers with a diameter of 70 to 100 nm, respectively. Studies reported that the prepared nanoparticles were highly used for food packaging due to hydrophobicity and thermal and tensile properties.[189]

One pot-assisted silver-based MOF synthesis *via* CS crosslinking was proposed for fresh fruit keeping. The one-step preparation of Ag-MOFs@CS suspension with improved antibacterial properties. The interaction of silver ions with CS's NH_2 and hydroxyl groups helps grow Ag-MOFs in the prepared matrix, which improves the effective dispersion and stabilization of Ag-MOFs and minimizes the release of Ag ions. The NH_2 and OH of the CS interacted with the silver MOFs strengthening the aqueous stability and minimizing the silver toxicity. The weight of the untreated strawberries declined by 50%, and the sprayed CS/MOFs retained more than 70% of their initial weight. The problems related to food safety are also minimized *via* washability.[190]

The CS/MOFs possess potential applications due to their composition, structure and ability to form any shape. The major challenges to be addressed to meet large-scale food packaging applications are listed below:

● Further research is mandatory to predict the mechanical and functional features of CS/MOFs.

● Continuing research is mandatory to determine the level of hazard that CS/MOFs can cause, and studies on suitable materials can be selected for CS/MOFs packaging.

5.8 Medical applications of CS/MOF

CS/MOFs exhibited prominent applications in bio-medical fields due to their excellent antibacterial properties, environmental suitability and safety, biodegradability, biocompatibility and recyclability. The presence of the CS in CS/MOF minimizes the cytotoxicity of MOFs and hinders the penetration of metal ions into biological samples through isolation of metal ions.

5.8.1 Antibacterial applications. With the growing population, the effects of bacterial diseases are also rising, which causes extreme stress to human and animal health.[191] In recent years, several nanomaterials have shown potential capabilities against eliminating the resistances and growth of bacteria.[192] As per the reports, a few studies are also conducted for CS/MOFs for antibacterial applications. Fig. 16 indicates the antibacterial activity mechanism of CS/MOFs.

Asl *et al.* (2022) developed Cu(II)-MOF@polydimethylsiloxane (PDMS) nanocomposite sponges coated with CS *via* blending of Cu-MOF into the PDMS sponge, followed by CS coating on the sponge *via* dip-coating. The developed sponges displayed good antibacterial efficiency against *S. aureus* and *E. coli*. The decline in the number of viable cells of bacteria is also reported. The biological studies also stressed that the prepared material provided adequate surface adhesion of cells, proliferation and viability.[193] In the same year, MOF-derived ZnO/porous carbon-13X zeolite composite modified with CS and Ag nanoparticles was developed to study the antibacterial properties. Experimental studies reported that ZnO-MOFC/13X/CS/Ag displayed a high antibacterial activity depending on the inhibition zone diameter of 14.5 and 1.5 mm on both *S. aureus* and *E. coli*. The ZnO-MOFC/13X/CS/Ag demonstrated a higher surface area.[194]

Wang *et al.* (2020) incorporated Cu-MOF (HKUST-1) with electrospun CS/PVA fibers using the electrospinning method. HKUST-1/CS/PVA fibers displayed phenomenal antibacterial activity towards *S. aureus* and *E. coli* with an efficiency of 99%. The cytotoxicity test proved biocompatibility and cell

Fig. 16 Mechanism of antibacterial properties of CS/MOF. The mechanism includes three pathways of metal ion release, accumulation in the cell wall, and linker release. This pathway causes enzyme disruption, cellular content mass leakage, and DNA and cell wall disruption.

adhesion.[195] Zhang *et al.* (2021) described the ZIF/CS prepared by the *in situ* method to enhance the antibacterial effect. The synergistic interaction between the ZIF and CS strengthened the antibacterial effect more than its pristine form. The inhibitory rate for *S. aureus* and *E. coli* reaches 96 and 100% within 15 hours. The CS/ZIF composite could destroy the bacterial cell, and internal nucleic acid leakage and protein leads to an effective antibacterial effect. The HKUST-1/CS/PVA fibers exhibited higher stability for at least five days.[196]

The UiO-66-NH$_2$ MOF nanoparticles with peroxidase and oxidase mimetic activities were blended with CS. The UiO-66-NH$_2$/CS membrane exhibited peroxidase-mimicking behavior under peroxide, causing better antibacterial properties against *Escherichia coli*. The advantages of this membrane are its high stability, compatibility and hydrophilicity.[197]

Overall, CS/MOFs exhibited prominent antibacterial properties. However, most studies were conducted on *S. aureus* and *E. coli*, respectively. In addition to Gram-positive and Gram-negative organisms, experiments must be conducted on various organisms to understand the study's scope. Studies must be conducted in both *in vivo* and *in vitro* modes to assess the activity of the CS/MOFs. Utilizing polysaccharides and chemical agents can increase the activity of the CS/MOFs.

5.8.2 Drug delivery and therapeutic treatment. Drug delivery systems comprise one or more pharmacologically active compounds with a respective carrier. During the past decade, polymers have been extensively used in drug delivery, devices for drug encapsulation and controlled release. The CS/MOF is also adopted for drug delivery applications. CS exhibits several properties, such as safety, biodegradable, biocompatible, easy modification, *etc.*, making CS/MOF unique. It is expected that CS/MOFs will work well for cancer therapy and other therapeutic applications (see Fig. 17).

Dizaji *et al.* (2020) focused on the fabrication of PLGA/CS/MOF (ZIF-8 & MIL-101) nanofibers through electrospinning. The prepared PLGA/CS/MOF nanofibers were highly useful for the controlled release of paclitaxel against prostate cancer *via in vivo* and *in vitro* methods. The prostate loading capacity of the PLGA/CS/NaY, PLGA/CS/ZIF-8, PLGA/CS/ZSM-5, and PLGA/CS/MIL-101 are 81.2%, 91.2%, 83.9% and 87% respectively. The cell viability of the normal fibroblast cells treated with different samples was >85%, which highlights the lower cytotoxicity of the prepared carriers in normal cells and proves the biocompatibility of the nano-fibrous CS based MOF. A higher degree of drug release rate was observed in the acidic pH. The PLGA/CS/ZIF-8 loaded with paclitaxel reported 86% of cells are dead after three days.[198]

In another study, vancomycin, an antibiotic, was loaded into ZIF-8 nanocrystal for pH-controlled release. The ZIF-8/vancomycin was loaded into CS scaffolds to yield 3-D structures through wet spinning. The experimental studies reported that vancomycin loaded into ZIF-8 nanocrystals was released in pH control conditions from the CS scaffolds. Almost 70% of vancomycin was released in the 8th hour at a pH of 5.4. The scaffolds can act as a substitute for bone, and drug carriers may be used to treat infections like osteomyelitis.[199] Lin *et al.* (2020)
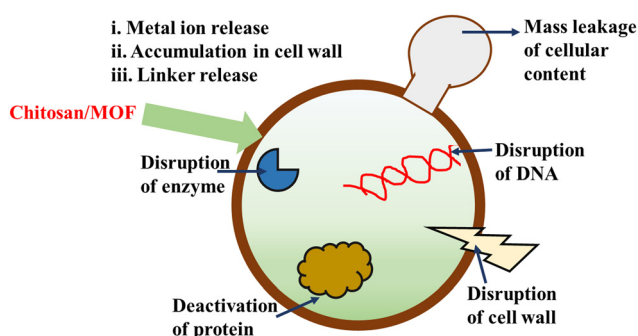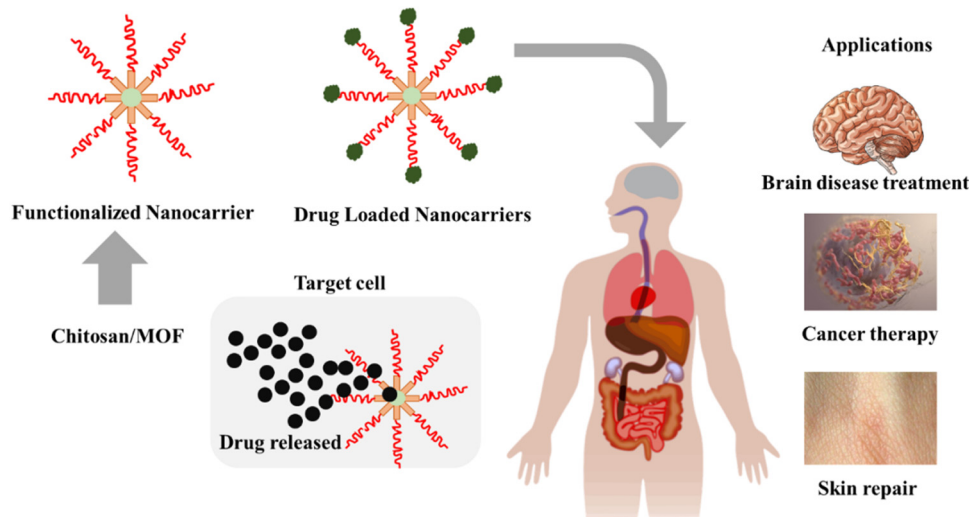
Fig. 17 Schematic representation of drug delivery using CS/MOFs and its potential applications in cancer therapy, skin repair, and brain disease treatment.

described the fabrication of carbon dot-embedded MOF@CS core–shell nanoparticles for drug delivery and vitro dual-mode imaging. Experimental studies were reported for doxorubicin as a model drug ($50 \ mg \ g^{-1}$). It is noticed that the doxorubicin was released suddenly at a pH of 3.8, and the extent of release greatly differed at a pH of 7.4. Cytotoxicity proved the biocompatibility and suitability of drug transportation in humans and animals.[200]

Cao *et al.* (2021) described the CS-coated biocompatible ZIF-90 for the delivery of the methotrexate. The methotrexate was loaded into ZIF-90 *via* a Schiff base reaction between the NH_2 in methotrexate and the aldehyde group of the imidazole-2-carboxaldehyde ligand with a loading of $250 \ mg \ g^{-1}$ (Fig. 18(a)). The outer layer modification of CS enhanced the pH responsiveness of the composite during drug release. The greater release of methotrexate under acidic conditions compared with under normal conditions under the normal environment. The cytotoxicity revealed that the prepared material CS@methotrexate@ZIF-90 minimized the growth of liver cancer HepG2 cells, prostate cancer DU145 cells and gastric cancer SGC7901 cells.[201] A group of researchers studied the therapeutic efficacy of 5-fluorouracil and gemcitabine with minimum influence using MIL-101. The impregnation effect was used to encapsulate 5-fluorouracil alone and with the gemcitabine in the MIL-101. Studies claimed all nanocarriers displayed anti-cancer activities and induced apoptosis in the MCF-7 cells. The cytotoxicity in the HUVEC cells is because of the chemotherapy drugs.[202]

Abdelhamid *et al.* (2020) discussed the carbonized CS encapsulated ZIF-8 for gene delivery. The mesoporous carbon materials were used as non-viral vectors to deliver genes using luciferase-expressing plasmid and splice-correction oligonucleotides. The illustration of surface modification of mesoporous carbon derived from CS-oligo nucleotides-two cell penetrating peptides and their gene delivery is indicated in Fig. 18(b). The carbon derived mesoporous carbon was effectively used as non-viral vectors for the delivery of two oligonucleotides named

luciferase-expressing plasmid and splice correction oligonucleotides. These materials exhibited low toxicity and biocompatibility. The transfection using mesoporous carbon with and without cell penetrating peptides. The phenomenal transfection efficiency is due to the synergistic effect of mesoporous carbon and cell penetrating peptides.[203]

In another study, folic acid and doxorubicin incorporated UiO-66 loaded onto carboxymethyl CS/polyethylene oxide/polyurethane core–shell membrane for the controlled release. The drug loading efficiency of folic acid and doxorubicin is 95%. The maximum cell death percentage of the fibres under 0.3, 0.5, and $0.8 \ mL \ h^{-1}$ are 82, 83, and 8% after 168, 240, and 240 hours respectively. Studies also proved the enhancement of the apoptotic nuclei and the suitability of the fibers for cancer treatment.[204]

The MOF-808 based on zirconium tricarboxylate decorated folic-acid conjugated CS was efficiently used to deliver quercetin. The cytotoxicity was explored using MTT assay against the folate-receptor-negative HEK-293 and folate receptor-positive MCF7 cells. The MTT assay affirmed the internalizing efficiency of the nanoparticles, additional to the cytotoxic and apoptosis-induced properties. The mechanism of selective internalization of the MOF-808 loaded quercetin by CS-folic acid through the receptor-mediate endocytosis. The key merits of this material include low-cost, easiness in fabrication, high stability, higher drug release in acidic tumor environments, and active tumor-targeting through its higher affinity of folic acids on the tumor cell surface.[205]

Table 3 summarizes different applications of CS/MOFs in drug delivery. The studies show that CS/MOFs can be highly used for drug delivery and therapeutic applications due to their biocompatibility and biodegradability. However, lower solubility and high swelling properties are undesirable for incorporating hydrophobic drugs. The immunological and toxicological profiles of CS/MOFs must be studied for the endurance of complete safety.
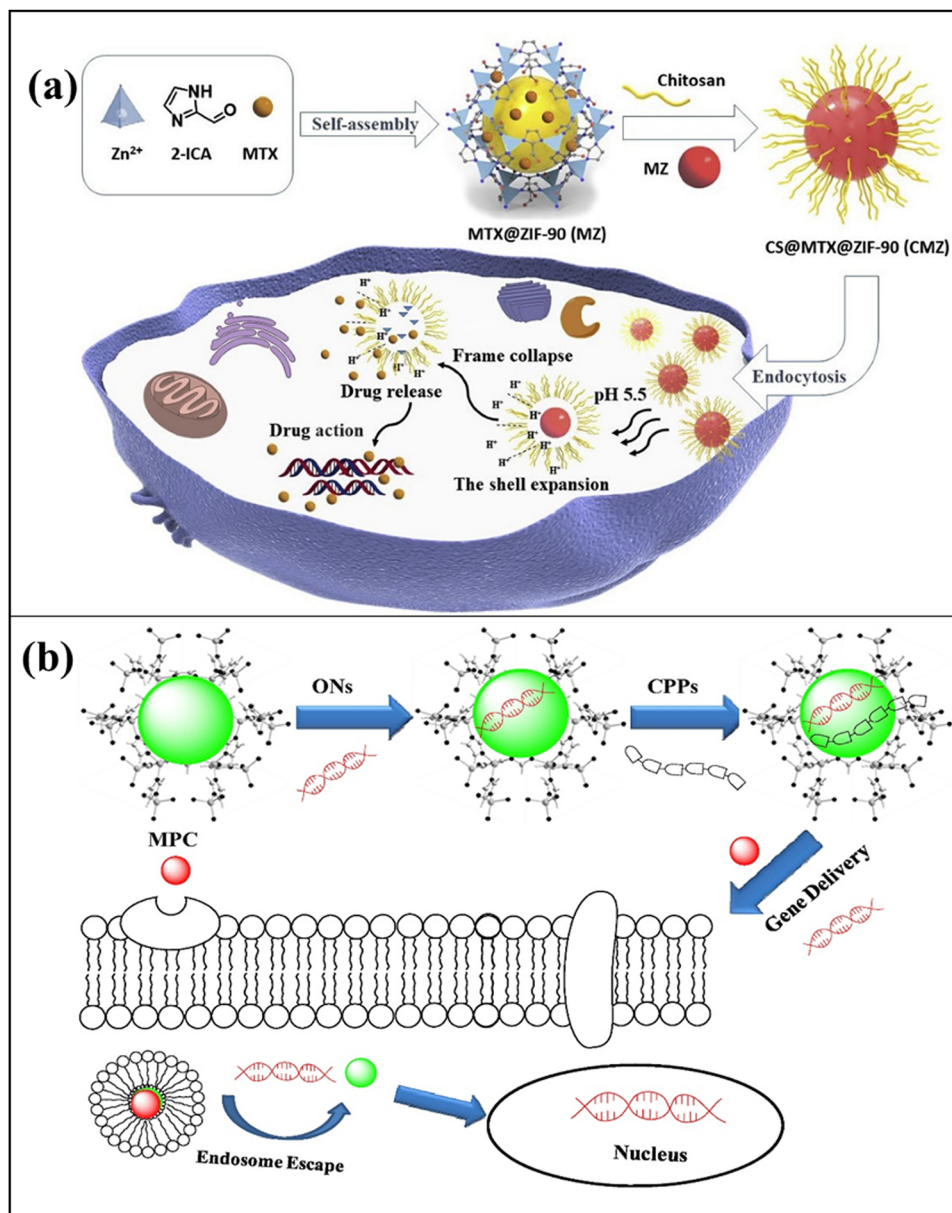
Fig. 18 (a) Diagrammatic representation of CS-coated biocompatible ZIF-90 for the delivery of the anticancer drug methotrexate. Reproduced with permission.[195] Copyright 2019, Elsevier. (b) Illustration of the synthesis of mesoporous carbon derived from CS-oligo nucleotides-two cell penetrating peptides and their gene delivery. Reproduced with permission.[203] Copyright 2020, Elsevier.

5.8.3 Tissue engineering. Bone tissue engineering and wound healing medicines are growing in regenerative medicine, which can be implemented by adopting different techniques such as nanotechnology, biomaterials, polymeric science and cell biology.

Khalili *et al.* (2020) focused on developing electroactive poly-(*p*-phenylene sulfide)/r-graphene oxide CS scaffolds for wound dressing applications. Studies reported a decline in the hydrogel swelling ratio from 800 to 200% *via* poly(*p*-phenylene sulfide)/r-graphene oxide inclusion. The prepared material exhibited good biocompatibility and cell attachment as well. The porous structure was a prominent method for improving cellular activity and growth. The developed scaffolds displayed a porosity of 85%.[214]

Recently, Karakecili *et al.* (2022) focused on the preparation of UiO-66 acting as a double actor in CS scaffolds for the osteogenesis promoter. Studies reported that the wet-electrospun CS scaffolds possessing fosfomycin-loaded UiO-66 nanocrystals exhibited a fiber mesh structure with integrated micro-scale fibers and extremely high mechanical strength. The CS scaffolds were biocompatible with MC3T3-E1 pre-osteoblast, up-regulated the osteogenesis-related gene expression, and boosted the extracellular matrix mineralization.[215]

6. Future prospects

CS/MOFs offer outstanding physical and chemical properties, which are mandatory for various applications. CS is commonly

Table 3   Drug delivery and therapeutic applications of CS/MOFs

Material	Form	Purpose	Observation	Application	Ref.
Fe_3O_4@Bio-MOF-coated folic acid-CS conjugate	Composite	Tumor targeted delivery of curcumin and 5-fluorouracil	Efficient drug loading capacity, controlled release of drugs, hemocompatibility and selective toxicity against cancerous cells	Cancer therapy	206
Ni/Ta core–shell MOF coated with folic acid-activated CS nanoparticles	Composite	Targeted delivery of doxorubicin and curcumin	Higher efficiency, high chemotherapeutic efficiency	Cancer therapy	207
PAA-CS/PU/MIL-53	Fibers	Co-delivery of paclitaxel and temozolomide against cancer cells	—	Cancer therapy	208
PVA/Ag-MOF and PV/CS bilayer	Hydrogel	Tissue engineering of lung scaffolds	Good antibacterial activity and poor biocompatibility	Lung scaffold	209
Carbon dots embedded magnetic nanoparticle@CS@MOF		Targeted doxorubicin delivery	pH-Responsive drug release	Cancer therapy	210
Cu(II) MOF@polydimethylsiloxane nanocomposite sponges coated with CS	Sponge	Tissue engineering	Reduced number of viable bacteria cells	Wound healing	193
MOF(HKUST-1) CS/PVA	Membrane	Wound healing	The prepared material heals the wound and minimizes inflammation	Skin repair	195
CS/bio-MOF	Composite	Targeted delivery of doxorubicin	The maximum drug loading efficiency of 92%	Cancer therapy	211
Chitosan/bacterial cellulose supported silver MOFs	Composite	Wound healing	—	Tissue repair	212
CS/Al-MOF/GO	Composite	Drug delivery	Biodegradability	Cancer therapy	213

employed as a modulator, support and binder for MOFs. The CS/MOFs are highly porous with multi-functional groups. Major advantages of CS/MOFs include (i) easy formulation into any shape, (ii) high porosity, flexibility, and better stability, and (iii) biodegradability. Despite the progress in the fabrication methods of CS/MOFs, some challenges must be addressed as follows:

(i) Complications in attaining ordered crystalline materials and predicting their topologies due to the poor symmetry of the bio-ligands.

(ii) Difficulty in maintaining porosity and open active sites in CS–MOFs.

(iii) Relatively harder to attain stability under relatively humid conditions.

• CS has a lower solubility in water, a major challenge in forming CS/MOFs materials. It is ascribed to the transformation of CS into a water-soluble form, which is highly beneficial during the fabrication of nanocomposites.

• All the MOFs do not exhibit the same mechanical strength. For example, HKUST displays a much lower mechanical strength. So, materials like graphene oxide and reduced graphene oxide can be blended into CS/HKUST to ensure the mechanical strength. However, low-cost materials can be used instead of graphene oxides for the endurance of mechanical stability.

• The structural stability of the CS/MOFs can be further increased *via* post-preparation modification which is beneficial for introducing several properties like the enhancement of porosity, number of catalytic sites, *etc.* Structural stability can be achieved *via*

(a) functionalization of the polysaccharides cross-linker.

(b) adopting covalent functionalization as a post-synthetic tool for modifying CS/MOFs. The combination of post-treatment methods can achieve the desired properties. Based on

their properties, the post-synthetic modification for CS/MOFs must be selected.

• The CS/MOFs demonstrated several applications in energy, environment and medicine. In previous years, several studies were reported for preparing CS/MOFs. The basic relationship between the highly complex structures and the properties needs further research. Very minimal research is conducted in supercapacitors, fuel cells, batteries, packaging, and drug delivery. So, apart from the experimental studies and theoretical calculations, computational modelling is beneficial for understanding the relationship between various MOF units.

• CS/MOF composites are also prone to fouling which minimizes the pore size and surface roughness and block the functional groups of CS/MOFs. Fabricating fouling-resistant CS/MOFs is important to ensure the efficiency of the material.

• The cytotoxicity studies of the CS/MOFs must be performed in-depth in the allied areas of bio-medical and genetic engineering.

• CS possesses a unique specialty as it can be formulated into any desired shape, such as film, foams, beads and 3D scaffolds, with the help of 3D printing technology. For the preparation, researchers must use low-cost chemicals to ensure economic feasibility.

• CS/MOF composites are prominent adsorbents that remove dyes, pesticides, heavy metals and pharmaceuticals. However, utilizing CS/MOFs on a large scale still requires extensive studies. The preparation routes of most of these composites are time-consuming, and the processes are uneconomical. From an industrial perspective, simple and alternative preparation routes must be developed using low-cost and minimum consumption of toxic chemicals. Furthermore, these materials must exhibit higher reusability and ease of recoverability. The cost-effective regeneration tool is always an asset for commercialization.

• Continuing research is necessary on the current applications of CS/MOFs in the fields of energy storage devices, sensors, food packaging, and biomedical applications.

7. Conclusions

CS/MOFs are an evolving group of hybrid materials in materials science. Combining biopolymer CS within the MOF structure enhances the structural flexibility and robustness and eventually improves the physical–chemical characteristics of the hybrid materials. The CS/MOFs exhibit biological compatibility and flexibility due to the existence of CS in their structure. Studies also proved that the ligand is critical in altering functional MOFs' size, shape, and fabrication. The different preparation routes of the CS/MOFs and the post-modification methods are emphasized in detail. The potential applications of CS/MOF in the environment, energy and medical field are thoroughly highlighted. Among different applications, CS/MOF is highly reported as an adsorbent, in which ZIF-8@CS/polyvinyl alcohol exhibited 1000 mg g^{-1} of adsorption capacity against the removal of malachite green. As a hybrid material, CS/MOF is promising in different areas, such as supercapacitors, fuel cells, and food packaging. It is also evident that the CS/MOF found its importance in drug delivery and tissue culture. The major challenges of CS/MOF are difficult to attain a well-ordered crystalline structure with greater porosity and open active sites which accounts for the efficiency of CS/MOFs. Despite the clarity of mechanisms, it can be anticipated that CS/MOFs are a highly smart and versatile material in the allied areas of materials science and technology.

Conflicts of interest

The authors declare no conflict of interest.

References

1 Q. L. Zhu and Q. Xu, *Chem. Soc. Rev.*, 2014, **43**, 5468.
2 H. N. Abdelhamid and A. P. Mathew, *Coord. Chem. Rev.*, 2022, **451**, 214263.
3 C. Vaitsis, G. Sourkouni and C. Argirusis, *Ultrason. Sonochem.*, 2019, **52**, 106.
4 J. Ren, X. Dyosiba, N. M. Musyoka, H. W. Langmi, M. Mathe and S. Liao, *Coord. Chem. Rev.*, 2017, **352**, 187.
5 X. Wang, P. She and Q. Zhang, *SmartMat*, 2021, **2**, 299.
6 D. Haldar, P. Duarah and M. K. Purkait, *Chemosphere*, 2020, **251**, 126388.
7 C. Du, Z. Zhang, G. Yu, H. Wu, H. Chen, L. Zhou, Y. Zhang, Y. Su, S. Tan, L. Yang, J. Song and S. Wang, *Chemosphere*, 2021, **272**, 129501.
8 Y. Shi, A. F. Yang, C. S. Cao and B. Zhao, *Coord. Chem. Rev.*, 2019, **390**, 50.
9 W. Zhou, J. Lu, K. Zhou, L. Yang, Y. Ke, Z. Tang and S. Chen, *Nano Energy*, 2016, **28**, 143.
10 T. T. Tung, M. T. Tran, J. F. Feller, M. Castro, T. Van Ngo, K. Hassan, M. J. Nine and D. Losic, *Carbon*, 2020, **159**, 333.
11 M. Kadhom and B. Deng, *Appl. Mater. Today*, 2018, **11**, 219.
12 X. Wen, Q. Zhang and J. Guan, *Coord. Chem. Rev.*, 2020, **409**, 213214.
13 B. Liu, H. Shioyama, H. Jiang, X. Zhang and Q. Xu, *Carbon*, 2010, **48**, 456.
14 C. L. Song, G. H. Li, Y. Yang, X. J. Hong, S. Huang, Q. F. Zheng, L. P. Si, M. Zhang and Y. P. Cai, *Chem. Eng. J.*, 2020, **381**, 122701.
15 M. Zhang, Y. Zheng, Y. Jin, D. Wang, G. Wang, X. Zhang, Y. Li and S. Lee, *Int. J. Biol. Macromol.*, 2022, **202**, 80.
16 S. Mallakpour, E. Nikkhoo and C. M. Hussain, *Coord. Chem. Rev.*, 2022, **451**, 214262.
17 M. R. Ramezani, Z. Ansari-Asl, E. Hoveizi and A. R. Kiasat, *Mater. Chem. Phys.*, 2019, **229**, 242.
18 Z. Gao, M. Hou, Y. Shi, L. Li, Q. Sun, S. Yang, Z. Jiang, W. Yang, Z. Zhang and W. Hu, *Chem. Sci.*, 2023, **14**, 6860.
19 J. Li, C. Wang, D. Wang, C. Yang, X. Cui, X. J. Gao and Z. Zhang, *J. Mater. Chem. A*, 2022, 20018–20023.
20 H. Musarurwa and N. T. Tavengwa, *Carbohydr. Polym.*, 2022, **275**, 118743.
21 J. Zhu, X. Chen, A. Q. Thang, F. Li, D. Chen, H. Geng, X. Rui and Q. Yan, *SmartMat*, 2022, **3**, 384.
22 H. S. Wang, Y. H. Wang and Y. Ding, *Nanoscale Adv.*, 2020, **2**, 3788.
23 S. S. Nadar, L. Vaidya, S. Maurya and V. K. Rathod, *Coord. Chem. Rev.*, 2019, **396**, 1.
24 R. S. Forgan, *Encycl. Inorg. Bioinorg. Chem.*, 2014, 1.
25 H. Musarurwa and N. T. Tavengwa, *Carbohydr. Polym.*, 2022, **283**, 119153.
26 A. Leudjo Taka, M. J. Klink, X. Yangkou Mbianda and E. B. Naidoo, *Carbohydr. Polym.*, 2021, **255**, 117398.
27 P. Mohammadzadeh Pakdel and S. J. Peighambardoust, *Carbohydr. Polym.*, 2018, **201**, 264.
28 R. Priyadarshi and J. W. Rhim, *Innov. Food Sci. Emerging Technol.*, 2020, **62**, 102346.
29 S. Bej, H. Sarma, M. Ghosh and P. Banerjee, *Environ. Pollut.*, 2023, **323**, 121278.
30 A. Balakrishnan, S. Appunni and K. Gopalram, *Int. J. Biol. Macromol.*, 2020, **161**, 282.
31 P. Sirajudheen, N. C. Poovathumkuzhi, S. Vigneshwaran, B. M. Chelaveettil and S. Meenakshi, *Carbohydr. Polym.*, 2021, **273**, 118604.
32 S. K. Shukla, A. K. Mishra, O. A. Arotiba and B. B. Mamba, *Int. J. Biol. Macromol.*, 2013, **59**, 46.
33 A. Ali and S. Ahmed, *Int. J. Biol. Macromol.*, 2018, **109**, 273.
34 S. A. Qamar, M. Ashiq, M. Jahangeer, A. Riasat and M. Bilal, *Case Stud. Chem. Environ. Eng.*, 2020, **2**, 100021.
35 M. Vakili, S. Deng, G. Cagnetta, W. Wang, P. Meng, D. Liu and G. Yu, *Sep. Purif. Technol.*, 2019, **224**, 373.
36 M. N. Ravi Kumar, *React. Funct. Polym.*, 2000, **46**, 1.
37 V. Vendramin, G. Spinato and S. Vincenzi, *Appl. Sci.*, 2021, **11**, 1.
38 F. Zouaoui, S. Bourouina-Bacha, M. Bourouina, N. Jaffrezic-Renault, N. Zine and A. Errachid, *TrAC, Trends Anal. Chem.*, 2020, **130**, 115982.

39 S. G. Roy and P. De, *J. Appl. Polym. Sci.*, 2014, **131**, 1.

40 M. Dash, F. Chiellini, R. M. Ottenbrite and E. Chiellini, *Prog. Polym. Sci.*, 2011, **36**, 981.

41 P. S. Bakshi, D. Selvakumar, K. Kadirvelu and N. S. Kumar, *Int. J. Biol. Macromol.*, 2020, **150**, 1072.

42 P. Sirajudheen and S. Meenakshi, *Mater. Today Proc.*, 2020, **27**, 318.

43 S. Appunni, M. P. Rajesh and S. Prabhakar, *Carbohydr. Polym.*, 2016, **147**, 525.

44 M. Hasmath Farzana and S. Meenakshi, *Int. J. Biol. Macromol.*, 2015, **72**, 1265.

45 F. S. Rezaei, F. Sharifianjazi, A. Esmaeilkhanian and E. Salehi, *Carbohydr. Polym.*, 2021, **273**, 118631.

46 Q. Zheng, D. Qin, R. Wang, W. Yan, W. Zhao, S. Shen, S. Huang, D. Cheng, C. Zhao and Z. Zhang, *Int. J. Biol. Macromol.*, 2022, **220**, 193.

47 N. Morin-Crini, E. Lichtfouse, G. Torri and G. Crini, *Environ. Chem. Lett.*, 2019, **17**, 1667.

48 S. Sakulwech, N. Lourith, U. Ruktanonchai and M. Kanlayavattanakul, *Asian J. Pharm. Sci.*, 2018, **13**, 498.

49 M. Escamilla-García, G. Calderón-Domínguez, J. J. Chanona-Pérez, R. R. Farrera-Rebollo, J. A. Andraca-Adame, I. Arzate-Vázquez, J. V. Mendez-Mendez and L. A. Moreno-Ruiz, *Int. J. Biol. Macromol.*, 2013, **61**, 196.

50 W. Chen, L. Du and C. Wu, *Met. Fram. Biomed. Appl.*, 2020, 141.

51 N. Manousi, D. A. Giannakoudakis, E. Rosenberg and G. A. Zachariadis, *Molecules*, 2019, **24**, 1.

52 J. Annamalai, P. Murugan, D. Ganapathy, D. Nallaswamy, R. Atchudan, S. Arya, A. Khosla, S. Barathi and A. K. Sundramoorthy, *Chemosphere*, 2022, **298**, 134184.

53 A. Al-Othman, M. Tawalbeh, O. Temsah and M. Al-Murisi, *Encycl. Smart Mater.*, 2022, 535.

54 R. Ediati, W. Aulia, B. A. Nikmatin, A. R. P. Hidayat, U. M. Fitriana, C. Muarifah, D. O. Sulistiono, F. Martak and D. Prasetyoko, *Mater. Today Chem.*, 2021, **21**, 100533.

55 Y. Pan, X. Hu, M. Bao, F. Li, Y. Li and J. Lu, *Sep. Purif. Technol.*, 2021, **279**, 119661.

56 P. A. Shinde, M. A. Abdelkareem, E. T. Sayed, K. Elsaid and A. G. Olabi, *Encycl. Smart Mater.*, 2022, 414.

57 V. Shrivastav, S. Sundriyal, P. Goel, H. Kaur, S. K. Tuteja, K. Vikrant, K. H. Kim, U. K. Tiwari and A. Deep, *Coord. Chem. Rev.*, 2019, **393**, 48.

58 S. Keskin and S. Kizilel, *Ind. Eng. Chem. Res.*, 2011, **50**, 1799.

59 B. Chen, Z. Yang, Y. Zhu and Y. Xia, *J. Mater. Chem. A*, 2014, **2**, 16811.

60 J. Chen, J. Ouyang, W. Chen, Z. Zheng, Z. Yang, Z. Liu and L. Zhou, *Chem. Eng. J.*, 2022, **431**, 134045.

61 Q. Liu, H. Yu, F. Zeng, X. Li, J. Sun, C. Li, H. Lin and Z. Su, *Carbohydr. Polym.*, 2021, **255**, 117402.

62 S. Gautam, H. Agrawal, M. Thakur, A. Akbari, H. Sharda, R. Kaur and M. Amini, *J. Environ. Chem. Eng.*, 2020, **8**, 103726.

63 P. Silva, S. M. F. Vilela, J. P. C. Tomé and F. A. Almeida Paz, *Chem. Soc. Rev.*, 2015, **44**, 6774.

64 T. R. Cook, Y. R. Zheng and P. J. Stang, *Chem. Rev.*, 2013, **113**, 734.

65 S. El Hankari, M. Bousmina and A. El Kadib, *Prog. Mater. Sci.*, 2019, **106**, 100579.

66 K. Kim, S. Lee, E. Jin, L. Palanikumar, J. H. Lee, J. C. Kim, J. S. Nam, B. Jana, T. H. Kwon, S. K. Kwak, W. Choe and J. H. Ryu, *ACS Appl. Mater. Interfaces*, 2019, **11**, 27512.

67 H. Nabipour, M. Mozafari and Y. Hu, *Met. Fram. Biomed. Appl.*, 2020, 321.

68 M. da Silva Pinto, C. A. Sierra-Avila and J. P. Hinestroza, *Cellulose*, 2012, **19**, 1771.

69 K. Tu, Y. Ding and T. Keplinger, *Carbohydr. Polym.*, 2022, **291**, 119539.

70 O. Shekhah, *Materials*, 2010, **3**, 1302.

71 X. F. Zhang, Z. Wang, M. Ding, Y. Feng and J. Yao, *J. Mater. Chem. A*, 2021, **9**, 23353.

72 A. Kumar, G. Sharma, M. Naushad, A. H. Al-Muhtaseb, A. García-Peñas, G. T. Mola, C. Si and F. J. Stadler, *Chem. Eng. J.*, 2020, **382**, 122937.

73 A. Balakrishnan, S. Appunni, M. Chinthala and D. V. N. Vo, *Environ. Chem. Lett.*, 2022, **20**, 3071.

74 A. Jandyal, I. Chaturvedi, I. Wazir, A. Raina and M. I. Ul Haq, *Sustainable Oper. Comput.*, 2022, **3**, 33.

75 L. Bergamonti, C. Bergonzi, C. Graiff, P. P. Lottici, R. Bettini and L. Elviri, *Water Res.*, 2019, **163**, 114841.

76 L. R. Yadav, S. V. Chandran, K. Lavanya and N. Selvamurugan, *Int. J. Biol. Macromol.*, 2021, **183**, 1925.

77 R. Jose Varghese, E. H. M. Sakho, S. Parani, S. Thomas, O. S. Oluwafemi and J. Wu, *Nanomater. Sol. Cell Appl.*, 2019, 75.

78 P. Davoodi, E. L. Gill, W. Wang and Y. Y. Shery Huang, *Biomed. Appl. Electrospinning Electrospraying*, 2021, 45.

79 A. Sharma, M. Thakur, M. Bhattacharya, T. Mandal and S. Goswami, *Biotechnol. Rep.*, 2019, **21**, e00316.

80 M. Patel, R. Kumar, K. Kishor, T. Mlsna, C. U. Pittman and D. Mohan, *Chem. Rev.*, 2019, **119**, 3510.

81 M. Ponnuchamy, A. Kapoor, P. Senthil Kumar, D.-V. N. Vo, A. Balakrishnan, M. Mariam Jacob and P. Sivaraman, *Environ. Chem. Lett.*, 2021, **19**, 2425.

82 A. Balakrishnan, M. Ponnuchamy, A. Kapoor and P. Sivaraman, *Legacy and Emerging Contaminants in Water and Wastewater. Emerging Contaminants and Associated Treatment Technologies*, Springer, 2022, pp. 231–261.

83 G. Crini and E. Lichtfouse, *Environ. Chem. Lett.*, 2019, **17**, 145.

84 A. Balakrishnan, M. Sillanpää, M. M. Jacob and D.-V. N. Vo, *Environ. Res.*, 2022, **213**, 113613.

85 A. Gürses, M. Açıkyıldız, K. Güneş and M. S. Gürses, *Dyes and Pigments: Their Structure and Properties*, in Dyes and Pigments, Springer, 2016, pp. 13–29.

86 A. Balakrishnan, M. Chinthala and R. K. Polagani, *Carbohydr. Polym.*, 2023, 121420.

87 M. Farhan Hanafi and N. Sapawe, *Mater. Today Proc.*, 2020, **31**, A141.

88 M. Ramesh and A. Muthuraman, *Nat. Artif. Flavor. Agents Food Dye*, 2018, 1.

89 J. Sharma, S. Sharma and V. Soni, *Reg. Stud. Mar. Sci.*, 2021, **45**, 101802.

90 A. Tkaczyk, K. Mitrowska and A. Posyniak, *Sci. Total Environ.*, 2020, **717**, 137222.

91 M. Khajavian, S. Shahsavarifar, E. Salehi, V. Vatanpour, M. Masteri-Farahani, F. Ghaffari and S. A. Tabatabaei, *Chem. Eng. Res. Des.*, 2021, **175**, 131.

92 Z. Zhang, J. Hu, X. Tian, F. Guo, C. Wang, J. Zhang and M. Jiang, *Appl. Surf. Sci.*, 2022, **599**, 153974.

93 W. Zhang, P. Sun, X. Wang, X. Zhang, L. Ran, Q. Zhao, B. Zou, L. Zhou and Z. Ye, *Mater. Today Commun.*, 2022, **31**, 103601.

94 F. Ahmadijokani, H. Molavi, A. Bahi, S. Wuttke, M. Kamkar, O. J. Rojas, F. Ko and M. Arjmand, *Chem. Eng. J.*, 2023, **457**, 141176.

95 Z. Chen, Z. B. Zhang, J. Zeng, Z. J. Zhang, S. Ma, C. M. Tang and J. Q. Xu, *Carbohydr. Polym.*, 2023, **299**, 120079.

96 D. Kanakaraju, B. D. Glass and M. Oelgemöller, *J. Environ. Manage.*, 2018, **219**, 189.

97 J. Wang and S. Wang, *J. Environ. Manage.*, 2016, **182**, 620.

98 E. P. Ambrosio-Albuquerque, L. F. Cusioli, R. Bergamasco, A. A. Sinópolis Gigliolli, L. Lupepsa, B. R. Paupitz, P. A. Barbieri, L. A. Borin-Carvalho and A. L. de Brito Portela-Castro, *Environ. Toxicol. Pharmacol.*, 2021, **83**, 103588.

99 V. Burke, D. Richter, J. Greskowiak, A. Mehrtens, L. Schulz and G. Massmann, *Water Environ. Res.*, 2016, **88**, 652.

100 L. Huang, R. Shen and Q. Shuai, *J. Environ. Manage.*, 2021, **277**, 111389.

101 A. Balakrishnan, E. S. Kunnel, R. Sasidharan, M. Chinthala and A. Kumar, *Chem. Eng. J.*, 2023, 146163.

102 R. Vardhan Patel and A. Yadav, *J. Mol. Struct.*, 2022, **1252**, 132128.

103 N. Zhuo, Y. Lan, W. Yang, Z. Yang, X. Li, X. Zhou, Y. Liu, J. Shen and X. Zhang, *Sep. Purif. Technol.*, 2017, **177**, 272.

104 X. Jia, B. Zhang, C. Chen, X. Fu and Q. Huang, *Carbohydr. Polym.*, 2021, **253**, 117305.

105 R. Zhao, T. Ma, S. Zhao, H. Rong, Y. Tian and G. Zhu, *Chem. Eng. J.*, 2020, **382**, 122893.

106 X. Chen, M. F. Hossain, C. Duan, J. Lu, Y. F. Tsang, M. S. Islam and Y. Zhou, *Chemosphere*, 2022, **307**, 135545.

107 M. Zaynab, R. Al-Yahyai, A. Ameen, Y. Sharif, L. Ali, M. Fatima, K. A. Khan and S. Li, *J. King Saud Univ. – Sci.*, 2022, **34**, 101653.

108 S. Zhong Hu, T. Huang, N. Zhang, Y. Zhou Lei and Y. Wang, *Carbohydr. Polym.*, 2022, **277**, 118809.

109 Z. Huang, C. Xiong, L. Ying, W. Wang, S. Wang, J. Ding and J. Lu, *Chem. Eng. J.*, 2022, **449**, 137722.

110 X. Zhu, J. Tong, L. Zhu and D. Pan, *Int. J. Biol. Macromol.*, 2022, **205**, 473.

111 H. Gul Zaman, L. Baloo, S. R. Kutty, K. Aziz, M. Altaf, A. Ashraf and F. Aziz, *Environ. Sci. Pollut. Res.*, 2023, **30**, 6216.

112 S. Wang, Y. Liu, Y. Hu and W. Shen, *Int. J. Biol. Macromol.*, 2023, **226**, 1054.

113 Z. Luo, H. Chen, S. Wu, C. Yang and J. Cheng, *Chemosphere*, 2019, **237**, 124493.

114 H. Motaghi, P. Arabkhani, M. Parvinnia and A. Asfaram, *Sep. Purif. Technol.*, 2022, **284**, 120258.

115 V. N. Le, T. N. Tu and J. Kim, *Sep. Purif. Technol.*, 2023, **306**, 122718.

116 X. Huang, S. Feng, G. Zhu, W. Zheng, C. Shao, N. Zhou and Q. Meng, *Int. J. Biol. Macromol.*, 2020, **149**, 882.

117 S. Yang, Y. Wang, H. Li, Y. Zhan, X. Ding, M. Wang, X. Wang and L. Xiao, *J. Porous Mater.*, 2021, **28**, 29.

118 N. M. Mahmoodi, M. Oveisi, A. Taghizadeh and M. Taghizadeh, *Carbohydr. Polym.*, 2020, **227**, 115364.

119 Y. Jin, Y. Li, Q. Du, B. Chen, K. Chen, Y. Zhang, M. Wang, Y. Sun, S. Zhao, Z. Jing, J. Wang, X. Pi and Y. Q. Wang, *Microporous Mesoporous Mater.*, 2023, **348**, 112404.

120 C. Niu, N. Zhang, C. Hu, C. Zhang, H. Zhang and Y. Xing, *Carbohydr. Polym.*, 2021, **258**, 117644.

121 L. Liu, Y. Ma, W. Yang, C. Chen, M. Li, D. Lin and Q. Pan, *New J. Chem.*, 2020, **44**, 15459.

122 Y. Wang, K. Wang, J. Lin, L. Xiao and X. Wang, *Int. J. Biol. Macromol.*, 2020, **165**, 2684.

123 L. Liu, J. Ge, L. T. Yang, X. Jiang and L. G. Qiu, *J. Porous Mater.*, 2016, **23**, 1363.

124 L. Wen, X. Chen, C. Chen, R. Yang, M. Gong, Y. Zhang and Q. Fu, *Arabian J. Chem.*, 2020, **13**, 5669.

125 Y. Ma, D. You, Y. Fang, J. Luo, Q. Pan, Y. Liu, F. Wang and W. Yang, *Sep. Purif. Technol.*, 2022, **294**, 121223.

126 D. Li, X. Tian, Z. Wang, Z. Guan, X. Li, H. Qiao, H. Ke, L. Luo and Q. Wei, *Chem. Eng. J.*, 2020, **383**, 123127.

127 A. M. Omer, E. M. Abd El-Monaem, M. M. Abd El-Latif, G. M. El-Subruiti and A. S. Eltaweil, *Carbohydr. Polym.*, 2021, **265**, 118084.

128 T. Chang, H. Lv, M. Tan, S. Zheng, W. B. Gao, B. Wang, Q. Zhao and B. Zhao, *J. Sol-Gel Sci. Technol.*, 2022, **103**, 730.

129 C. Wang, Q. Sun, L. Zhang, T. Su and Y. Yang, *J. Environ. Chem. Eng.*, 2022, **10**, 107911.

130 E. Bahmani, S. Koushkbaghi, M. Darabi, A. ZabihiSahebi, A. Askari and M. Irani, *Carbohydr. Polym.*, 2019, **224**, 115148.

131 N. Xiong, P. Wan, G. Zhu, F. Xie, S. Xu, C. Zhu and A. S. Hursthouse, *Sep. Purif. Technol.*, 2020, **236**, 116266.

132 L. Liu, W. Yang, D. Gu, X. Zhao and Q. Pan, *Front. Chem.*, 2019, **7**, 1.

133 Y. Wei, R. Zou, Y. Xia, Z. Wang, W. Yang, J. Luo and C. Liu, *Mater. Today Chem.*, 2022, **26**, 101091.

134 X. Guo, H. Yang, Q. Liu, J. Liu, R. Chen, H. Zhang, J. Yu, M. Zhang, R. Li and J. Wang, *Chem. Eng. J.*, 2020, **382**, 122850.

135 F. M. Valadi, S. Shahsavari, E. Akbarzadeh and M. R. Gholami, *Carbohydr. Polym.*, 2022, **288**, 119383.

136 H. Zhao, J. Sun, Y. Du, M. Zhang, Z. Yang, J. Su, X. Peng, X. Liu, G. Sun and Y. Cui, *J. Solid State Chem.*, 2023, **322**, 123928.

137 X. Yan and H. Ge, *Int. J. Biol. Macromol.*, 2023, **232**, 123329.

138 T. R. Anderson, E. Hawkins and P. D. Jones, *Endeavour*, 2016, **40**, 178.

139 C. D. Keeling, *Proc. Natl. Acad. Sci. U. S. A.*, 1997, **94**, 8273.

140 M. C. Singo, X. C. Molepo, O. O. Oluwasina and M. O. Daramola, *Energy Procedia*, 2017, **114**, 2429.

141 P. Jiamjirangkul, T. Inprasit, V. Intasanta and A. Pangon, *Chem. Eng. Sci.*, 2020, **221**, 115650.

142 J. Nie, H. Xie, M. Zhang, J. Liang, S. Nie and W. Han, *Carbohydr. Polym.*, 2020, **250**, 116955.

143 D. Hao, B. Fu, J. Zhou and J. Liu, *Sep. Purif. Technol.*, 2022, **294**, 120927.

144 C. Li, N. He, X. Zhao, X. Zhang, W. Li, X. Zhao and Y. Qiao, *Chem. Sel.*, 2022, **7**, e202103927.

145 W. Zhang, T. Huang, Y. Ren, Y. Wang, R. Yu, J. Wang and Q. Tu, *Int. J. Biol. Macromol.*, 2021, **193**, 2243.

146 D. K. Yoo, H. C. Woo and S. H. Jhung, *Coord. Chem. Rev.*, 2020, **422**, 2213477.

147 W. Pan, J. P. Wang, X. B. Sun, X. X. Wang, J. Yong Jiang, Z. G. Zhang, P. Li, C. H. Qu, Y. Z. Long and G. F. Yu, *J. Cleaner Prod.*, 2021, **291**, 125270.

148 A. Balakrishnan, K. Gopalram and S. Appunni, *Environ. Sci. Pollut. Res.*, 2021, **28**, 33331.

149 M. S. Samuel, S. Suman, Venkateshkannan, E. Selvarajan, T. Mathimani and A. Pugazhendhi, *J. Photochem. Photobiol. B Biol.*, 2020, **204**, 111809.

150 S. Vigneshwaran, P. Sirajudheen, V. P. Sajna, C. M. Park and S. Meenakshi, *Environ. Sci. Pollut. Res.*, 2023, **30**, 24876.

151 F. Ghourchian, N. Motakef-Kazemi, E. Ghasemi and H. Ziyadi, *J. Environ. Chem. Eng.*, 2021, **9**, 106388.

152 J. Zhang, E. Ding, S. Xu, Z. Li, A. Fakhri and V. K. Gupta, *Int. J. Biol. Macromol.*, 2020, **164**, 1584.

153 S. Vigneshwaran, P. Sirajudheen, P. Karthikeyan, M. Nikitha, K. Ramkumar and S. Meenakshi, *J. Hazard. Mater.*, 2021, **406**, 124728.

154 Z. S. Zhao, Y. Zhang, T. Fang, Z. B. Han and F. S. Liang, *ACS Appl. Nano Mater.*, 2020, **3**, 6316.

155 M. Yousefian and Z. Rafiee, *Carbohydr. Polym.*, 2020, **228**, 115393.

156 G. Wang, J. Wang, Z. Chen and J. Hu, *Int. J. Biol. Macromol.*, 2022, **206**, 232.

157 X. H. Ma, Z. Yang, Z. K. Yao, Z. L. Xu and C. Y. Tang, *J. Membr. Sci*, 2017, **525**, 269.

158 X. Wang, Q. Wang, M. Zhao, L. Zhang, X. Ji, H. Sun, Y. Sun, Z. Ma, J. Xue and X. Gao, *Membranes*, 2022, **12**, 144.

159 P. Shi, X. Hu and M. DUan, *J. Cleaner Prod.*, 2021, **290**, 125794.

160 R. Lakra, M. Balakrishnan and S. Basu, *J. Environ. Chem. Eng.*, 2021, **9**, 105882.

161 X. Xu, Y. Hartanto, D. Nikolaeva, Z. He, S. Chergaoui and P. Luis, *Sep. Purif. Technol.*, 2022, **293**, 121085.

162 H. Zhu, R. Li, G. Liu, Y. Pan, J. Li, Z. Wang, Y. Guo, G. Liu and W. Jin, *J. Membr. Sci.*, 2022, **652**, 120473.

163 M. Vinu, D. Senthil Raja, Y. C. Jiang, T. Y. Liu, Y. Y. Xie, Y. F. Lin, C. C. Yang, C. H. Lin, S. M. Alshehri, T. Ahamad, R. R. Salunkhe, Y. Yamauchi, Y. H. Deng and K. C. W. Wu, *J. Taiwan Inst. Chem. Eng.*, 2018, **83**, 143.

164 C. Casado-Coterillo, A. Fernández-Barquín, B. Zornoza, C. Téllez, J. Coronas and Á. Irabien, *RSC Adv.*, 2015, **5**, 102350.

165 X. Zhu, Z. Yu, H. Zeng, X. Feng, Y. Liu, K. Cao, X. Li and R. Long, *J. Appl. Polym. Sci.*, 2021, **138**, 50765.

166 R. Si, H. Luo, T. Zhang and J. Pu, *Int. J. Biol. Macromol.*, 2023, **238**, 124008.

167 Q. Li, Q. Liu, J. Zhao, Y. Hua, J. Sun, J. Duan and W. Jin, *J. Membr. Sci.*, 2017, **544**, 68.

168 S. Fazlifard, T. Mohammadi and O. Bakhtiari, *Chem. Eng. Technol.*, 2017, **40**, 648.

169 C. H. Kang, Y. F. Lin, Y. S. Huang, K. L. Tung, K. S. Chang, J. T. Chen, W. S. Hung, K. R. Lee and J. Y. Lai, *J. Membr. Sci.*, 2013, **438**, 105.

170 D. D. Kachhadiya and Z. V. P. Murthy, *J. Environ. Chem. Eng.*, 2023, **11**, 109307.

171 M. J. Neufeld, A. Lutzke, J. B. Tapia and M. M. Reynolds, *ACS Appl. Mater. Interfaces*, 2017, **9**, 5139.

172 M. Pishnnamazi, S. Koushkbaghi, S. S. Hosseini, M. Darabi, A. Yousefi and M. Irani, *J. Mol. Liq.*, 2020, **317**, 113934.

173 S. Jamshidifard, S. Koushkbaghi, S. Hosseini, S. Rezaei, A. Karamipour, A. Jafari Rad and M. Irani, *J. Hazard. Mater.*, 2019, **368**, 10.

174 M. Chinthala, A. Balakrishnan, P. Venkataraman, V. Manaswini Gowtham and R. K. Polagani, *Environ. Chem. Lett.*, 2021, **19**, 4415.

175 Poonam, K. Sharma, A. Arora and S. K. Tripathi, *J. Energy Storage*, 2019, **21**, 801.

176 A. Ehsani, M. Bigdeloo, F. Assefi, M. Kiamehr and R. Alizadeh, *Inorg. Chem. Commun.*, 2020, **115**, 107885.

177 S. Zhanng, M. Kitta and Q. Xu, *Chem. – Asian J.*, 2019, **14**, 3583.

178 Y. Han, P. Qi, S. Li, X. Feng, J. Zhou, H. Li, S. Su, X. Li and B. Wang, *Chem. Commun.*, 2014, **50**, 8057.

179 M. Wang, J. Zhang, X. Yi, X. Zhao, B. Liu and X. Liu, *Appl. Surf. Sci.*, 2020, **507**, 145166.

180 K. Divy, M. S. S. A. Saraswathi, A. Nagendran and D. Rana, *J. Appl. Polym. Sci*, 2022, **139**, e52829.

181 S. Zhao, Y. Yang, F. Zhong, W. Niu, Y. Liu, G. Zheng, H. Liu, J. Wang and Z. Xiao, *Polymer*, 2021, **226**, 123800.

182 H. S. Choi, X. Yang, G. Liu, D. S. Kim, J. H. Yang, J. H. Lee, S. O. Han, J. Lee and S. W. Kim, *J. Taiwan Inst. Chem. Eng.*, 2020, **113**, 1.

183 L. Huang, W. Huang, R. Shen and Q. Shuai, *Food Chem.*, 2020, **330**, 127212.

184 M. Miao, L. Mu, S. Cao, Y. Yang and X. Feng, *Carbohydr. Polym.*, 2022, **291**, 119587.

185 Y. Jiang, Z. Qin, F. Liang, J. Li, Y. Sun, X. Wang, P. Ma and D. Song, *J. Chromatogr. A*, 2021, **1638**, 461887.

186 H. Si, P. He, X. Wang, L. Li and X. Hou, *New J. Chem.*, 2022, **46**, 808.

187 A. Sridhar, M. Ponnuchamy, A. Kapoor and S. Prabhakar, *J. Hazard. Mater.*, 2022, **424**, 127432.

188 A. Sultana, A. Kathuria and K. K. Gaikwad, *Environ. Chem. Lett.*, 2022, **20**, 1479.

189 I. Kohsari, Z. Shariatinia and S. M. Pourmortazavi, *Int. J. Biol. Macromol.*, 2016, **91**, 778.

190 Y. Zhang, Z. Lin, Q. He, Y. Deng, F. Wei, C. Xu, L. Fu and B. Lin, *Appl. Surf. Sci.*, 2022, **571**, 151351.

191 D. M. Morens and A. S. Fauci, *PLoS Pathog.*, 2013, **9**, e1003467.

192 G. Wyszogrodzka, B. Marszałek, B. Gil and P. Dorozyński, *Drug Discov. Today*, 2016, **21**, 1009.

193 Z. Ansari-Asl, Z. Shahvali, R. Sacourbaravi, E. Hoveizi and E. Darabpour, *Microporous Mesoporous Mater.*, 2022, **336**, 111866.

194 E. Alrin, C. R. Tjampakasari and Y. K. Krisnandi, *Inorg. Chem. Commun.*, 2022, **144**, 109943.

195 S. Wang, F. Yan, P. Ren, Y. Li, Q. Wu, X. Fang, F. Chen and C. Wang, *Int. J. Biol. Macromol.*, 2020, **158**, 9.

196 M. Zhang, S. Ye, J. Wang, K. Yu, J. Cao, G. Li and X. Liao, *Int. J. Biol. Macromol.*, 2021, **186**, 639.

197 X. Wang, X. Zhou, K. Yang, Q. Li, R. Wan, G. Hu, J. Ye, Y. Zhang, J. He, H. Gu, Y. Yang and L. Zhu, *Biomater. Sci.*, 2021, **9**, 2647.

198 B. Faraji Dizaji, M. Hasani Azerbaijan, N. Sheisi, P. Goleij, T. Mirmajidi, F. Chogan, M. Irani and F. Sharafian, *Int. J. Biol. Macromol.*, 2020, **164**, 1461.

199 A. Karakeçili, B. Topuz, S. Korpayev and M. Erdek, *Mater. Sci. Eng., C*, 2019, **105**, 110098.

200 C. Lin, K. Sun, C. Zhang, T. Tan, M. Xu, M. Liu, C. Xu, Y. Wang, L. Li and A. Whittaker, *Microporous Mesoporous Mater.*, 2020, **293**, 109775.

201 X. X. Cao, S. L. Liu, J. S. Lu, Z. W. Zhang, G. Wang, Q. Chen and N. Lin, *J. Solid State Chem.*, 2021, **300**, 122259.

202 A. K. Resen, A. Atiroğlu, V. Atiroğlu, G. Guney Eskiler, I. H. Aziz, S. Kaleli and M. Özacar, *Int. J. Biol. Macromol.*, 2022, **198**, 175.

203 H. N. Abdelhamid, M. Dowaidar and Ü. Langel, *Microporous Mesoporous Mater.*, 2020, **302**, 110200.

204 A. Farboudi, K. Mahboobnia, F. Chogan, M. Karimi, A. Askari, S. Banihashem, S. Davaran and M. Irani, *Int. J. Biol. Macromol.*, 2020, **150**, 178.

205 M. Parsaei and K. Akhbari, *Inorg. Chem.*, 2022, **61**, 19354.

206 V. Nejadshafiee, H. Naeimi, B. Goliaei, B. Bigdeli, A. Sadighi, S. Dehghani, A. Lotfabadi, M. Hosseini, M. S. Nezamtaheri, M. Amanlou, M. Sharifzadeh and M. Khoobi, *Mater. Sci. Eng., C*, 2019, **99**, 805.

207 S. Sadat Jalaladdiny, A. Badoei-dalfard, Z. Karami and G. Sargazi, *J. Iran. Chem. Soc.*, 2022, **19**, 4287.

208 A. Bazzazzadeh, B. F. Dizaji, N. Kianinejad, A. Nouri and M. Irani, *Int. J. Pharm.*, 2020, **587**, 119674.

209 M. Zhang, G. Wang, X. Zhang, Y. Zheng, S. Lee, D. Wang and Y. Yang, *Polymers*, 2021, **13**, 1.

210 A. R. Chowdhuri, T. Singh, S. K. Ghosh and S. K. Sahu, *ACS Appl. Mater. Interfaces*, 2016, **8**, 16573.

211 R. Abazari, A. R. Mahjoub, F. Ataei, A. Morsali, C. L. Carpenter-Warren, K. Mehdizadeh and A. M. Z. Slawin, *Inorg. Chem.*, 2018, **57**, 13364.

212 M. Barjasteh, S. M. Dehnavi, S. Ahmadi Seyedkhani, S. Y. Rahnamaee and M. Golizadeh, *Surf. Interfaces*, 2023, **36**, 102631.

213 E. Aghazadeh Asl, M. Pooresmaeil and H. Namazi, *Mater. Chem. Phys.*, 2023, **293**, 126933.

214 R. Khalili, P. Zarrintaj, S. H. Jafari, H. Vahabi and M. R. Saeb, *Int. J. Biol. Macromol.*, 2020, **154**, 18.

215 A. Karakeçili, B. Topuz, F. Ş. Ersoy, T. Şahin, A. Günyakti and T. T. Demirtaş, *Biomater. Adv.*, 2022, **136**, 212757.